CONF-861080--3

SAND--86-0342C

DE86 014297

SAND86-0342C
The Use of Single - Cutter Data in the Analysis of PDC Bit Designs

David A. Glowka

Received by OSTI

AUG 1 5 1986

For presentation at:
61st Annual Technical Conference and Exhibition of
Society of Petroleum Engineers
New Orleans, LA
October 5-10, 1986

DISCLAIMER

This report was prepared as an account of work sponsored by an agency of the United S
Government. Neither the United States Government nor any agency thereof, nor any of
employees, makes any warranty, express or implied, or assumes any legal liability or res
bility for the accuracy, completeness, or usefulness of any information, apparatus, produ
process disclosed, or represents that its use would not infringe privately owned rights. I
ence herein to any specific commercial product, process, or service by trade name, trade
manufacturer, or otherwise does not necessarily constitute or imply its endorsement, r
mendation, or favoring by the United States Government or any agency thereof. The
and opinions of authors expressed herein do not necessarily state or reflect those o
United States Government or any agency thereof.

MASTER

DISTRIBUTION OF THIS DOCUMENT IS UNLIMITED

DISCLAIMER

This report was prepared as an account of work sponsored by an agency of the United States Government. Neither the United States Government nor any agency Thereof, nor any of their employees, makes any warranty, express or implied, or assumes any legal liability or responsibility for the accuracy, completeness, or usefulness of any information, apparatus, product, or process disclosed, or represents that its use would not infringe privately owned rights. Reference herein to any specific commercial product, process, or service by trade name, trademark, manufacturer, or otherwise does not necessarily constitute or imply its endorsement, recommendation, or favoring by the United States Government or any agency thereof. The views and opinions of authors expressed herein do not necessarily state or reflect those of the United States Government or any agency thereof.

DISCLAIMER

Portions of this document may be illegible in electronic image products. Images are produced from the best available original document.

ABSTRACT

A method is developed for predicting cutter forces, temperatures, and wear on PDC bits as well as integrated bit performance parameters such as weight-on-bit (WOB), drilling torque, and bit imbalance. A computer code called PDCWEAR has been developed to make this method available as a tool for general bit design. The method uses single-cutter data to provide a measure of rock drillability and employs theoretical considerations to account for interaction among closely spaced cutters on the bit. Experimental data are presented to establish the effects of cutter size and wearflat area on the forces that develop during rock cutting. Waterjet assistance is shown to significantly reduce cutting forces, thereby extending bit life and reducing WOB and torque requirements in hard rock. The effects of bit profile, cutter placement density, bit rotary speed, and wear mode on bit life and drilling performance are investigated.

INTRODUCTION

Research has been conducted for several years at Sandia National Laboratories to foster the development of PDC bits for geothermal drilling. This work has been directed toward the high-temperature, hard-rock drilling environment that is typically found near geothermal resources. We have strived, however, to interpret the results to make them generally applicable to drilling environments of interest to the petroleum industry as well.

Our previous experimental and theoretical studies suggest a strong dependence of PDC cutter wear rates on the frictional temperatures that develop at the cutter/rock interface [1,2]. The results indicate that above a critical wearflat temperature of approximately 350°C, wear mechanisms that greatly accelerate cutter wear become operative. Such thermally-accelerated wear can

---

References and illustrations at end of paper.

reduce bit life by one or two orders of magnitude, generally to an unacceptable level [3]. Below 350°C, wear is generally very low and is predominantly one of abrasion, without any apparent thermal effects. Abrasive wear is a strong function of the abrasiveness of the rock being cut and the stresses that develop at the cutter/rock interface. Designing and operating PDC bits to perform effectively within the constraints suggested by these concepts is the subject of this paper.

Models developed to predict cutter wearflat temperatures [1,4,5] and wear rates [2,3] require an estimate of the penetrating stress for each cutter of interest. This is the stress that develops normal to the cutter wearflat during drilling (see Fig. 1). Because of cutter interaction and the non-planar placement of cutters on a given bit body, accurately predicting the stresses for each cutter is not a trivial matter. This point is illustrated in Fig. 2, which shows a typical sequence of sharp cutting edge profiles for several cutters on the leading face of a PDC bit. These profiles are obtained during two revolutions of the bit as the cutters pass through a radial (x,z) plane containing the longitudinal axis of the bit. The shaded areas represent the steady-state cross-sectional areas of cut for each cutter, assuming that the cut profiles are the same as the cutter profiles. (In tests done with brittle rock at atmoshpheric pressure, this assumption was found to be valid [14].) Since the center of the cutters are all assumed to lie at the same longitudinal location on the bit body, the downward vertical displacement of one cutter profile relative to a preceding one is due entirely to the advancement of the bit as it rotates. The shape of the cross-sectional areas of cut are seen to be quite complex, even for such a simple bit geometry.

In a typical bit design, the cross-sectional areas of cut depend on the radial, circumferential, and longitudial distribution of cutters on the bit face and on the cutter wear patterns and bit penetration rate. Although it is possible to

duplicate some interaction patterns in the laboratory, it is clearly impractical in single-cutter tests to duplicate all the combinations of cutter wear and interaction that could be experienced by cutters in any given bit design.

The objective of this paper is to present an approach to calculating cutter penetrating stresses in general bit design. This approach is based on laboratory single-cutter force data that describe the inherent drillability of the cutter-rock combination and on analytical considerations that predict cutter interaction effects. The approach requires that single-cutter data be obtained under the same operating conditions as those for which performance prediction of the full PDC bit is to be made. The geometry of the cuts that provide these baseline drillability data, however, is simpler than the geometry of cuts obtained with an actual bit. The standard test cut chosen for this approach is a single cut on a flat rock surface.

It is possible to achieve this simple standard cut with most drag cutter testing machines currently in existence. Several machines are available for obtaining single cutter data under elevated, and in some cases distinct, borehole, confining, and pore pressures [6,7,8,9]. The approach developed in this paper offers a method for using such data to predict PDC bit performance under downhole pressure conditions. In addition, bit performance at atmospheric conditions can be predicted using single-cutter data obtained with machine tools such as modified mills, shapers, and lathes. Although atmospheric-pressure, full-scale bit tests do not provide an accurate quantitative measure of downhole bit performance, they are useful in comparing alternative bit designs and determining whether or not field or elevated-pressure lab tests may be warranted for a given design. Prediction of bit performance at atmospheric conditions would be similarly useful.

The potential for using moderate-pressure waterjets to extend the range of application of PDC cutters is also explored in this paper. Previous work by Hood [10,11] and others [12] with large cemented carbide cutters used in hard-rock mining applications has shown that cutter forces can be significantly reduced if waterjets are directed onto the rock surface immediately ahead of the cutter. Penetrating force reductions of 50% with 2500 psi jets and 75% with 9000 psi jets have been reported. Our previous analysis [13] indicates that if such reductions could be achieved downhole with PDC cutters, they would be sufficient to permit cutters to operate under more severe conditions and in significantly harder rocks, extending the applicability of PDC bits to more types of formations. This paper presents new data obtained with PDC cutters and cavitating jets that support that conclusion. The application of the cutter/waterjet technique in PDC bit design is also discussed.

This paper is a condensed version of Ref. 14. The referenced report presents further details, such as raw experimental data and a user's manual for the computer code PDCWEAR. The basic approach and all the pertinent equations are, however, developed and presented in the present paper.

EXPERIMENTAL PROCEDURE AND RESULTS

The data that must be obtained to provide a measure of drillability are the penetrating and drag forces, F and F_d, as a function of the depth of cut, δ. This depth is measured in the center of the cut and should generally cover the range 0.005 to 0.080 inches. These data must be obtained with one sharp and one worn cutter. Single cuts must be made on a smooth rock surface and must be separated from adjacent cuts so that no interaction occurs between cut profiles. Once these data are obtained, correlations of the following forms are possible:

$$F/A_w = C_1\delta^{n1} \qquad (1)$$

$$F = C_2\delta^{n2}\ , \qquad (2)$$

where the constants, C_1 and C_2, and exponents, n1 and n2, are determined from a least-squares fit of the data in log-log space. Previous work [3] demonstrated that these correlations can be used to predict penetrating forces during cutter interaction by substituting an effective depth of cut, δ_e, for δ. A more complete and generalized discussion of the effective-depth-of-cut concept is presented in a later section.

In our previous experimental work [3], we used a single cutter with a wearflat area that ranged from 0.030 to 0.040 in^2. Dry cuts in three rock types were made, and correlations of the form given in Eq. 1 were obtained. In order to explore the effects of wearflat area and waterjet assistance on this correlation, further data were obtained in the present study.

In this study, rock-cutting tests were conducted in two rock types with PDC cutters having various amounts of wear. Berea sandstone (UCS=7100 psi) and Sierra White granite (UCS=21,500 psi) were used in order to cover a wide range of rock properties such as strength, composition, and ductility. These rocks were previously used and are described in more detail in Ref. 3. Single-cutter forces were measured with a linear-traversing milling machine and a triaxial force transducer, as previously described [3]. Force samples made during each cut were averaged, and these mean values are reported.

Cutters in various stages of wear were used in an effort to determine the effects of wear on cutter forces. New PDC cutters with sharp edges were used, as were cutters with machine-ground, laboratory-worn, and field-worn wearflats. The machine-ground wearflats were produced by grinding new cutters in a direction parallel to the direction of cutter travel. Cutters with field-worn wearflats were removed from commercial bits that had been run in oil and gas wells. Laboratory-worn wearflats were obtained with a vertical milling machine. Long spiral cuts on a large specimen of Sierra White Granite were made to allow cutters to wear naturally.

Cutter wearflats were measured as follows. A piece of carbon paper was inserted between two sheets of plain paper and placed between the cutter and the flat rock surface. The cutter was then statically loaded to a penetrating force level typical of the level encountered in cutting tests with the same cutter and rock. The portion of the cutter wearflat that contacted the rock left a carbon impression on the plain paper. This

impression was overlain with a fine rectangular grid (1 mm x 1mm) and the area calculated by counting shaded blocks. Cutters with measured wearflats ranging from 0.016 to 0.040 in^2 were tested in this study. These and other measured wearflat dimensions are listed in Table I.

Two sizes of cutter were tested. Most cutters had compact diameters of 0.5 inch, the size that has been traditionally used in PDC bits. Also tested, both new and laboratory-worn, was a cutter having a compact diameter of 0.75 inch. All cutters had backrake angles of 20^o.

In the current study, the milling machine table was also fitted with a steel enclosure and a waterjet nozzle holder mounted ahead of the cutter. A profile of the nozzle holder and and its relationship to the cutter are shown in Fig. 3. The nozzle holder was designed so that the nozzle standoff distance, d_s, inclination angle, ϕ_n, and jet impingement distance, d_j, could be adjusted over limited ranges. Only one set of these parameters was actually used in the test program currently reported, as listed in the figure caption. These values were chosen to represent practical values that might be used in an actual PDC bit design.

The nozzles used in the test program were self-resonating, cavitating jet nozzles designed and fabricated by Tracor Hydronautics, Inc. under contract to Sandia National Laboratories [15]. The cavitation bubbles produced in these jets are created by the vaporization of liquid in the center of high velocity vortices that form in the jet shear zone. When these cavities collapse near a rock surface, high-speed microjets impact the rock surface with pressures on the order of 150 kpsi [16], substantially increasing rock erosion and cleaning rates over certain ranges in nozzle pressure drop [17]. Two nozzles were fabricated for the single-cutter tests: one optimized for a pressure drop of 2000 psi and the other for a pressure drop of 4500 psi. Both had orifice diameters of 0.1 inches. Cuts made with PDC cutters and jets operating at these elevated pressures were compared with identical cuts made with 80 psi jets and cuts made with no jets at all (i.e., dry).

Dry Non-Interacting Cuts

Shown in Fig. 4 are the measured penetrating stresses, F/A_w, plotted as a function of depth of cut for the worn cutters. The curves represent correlations of the form given in Eq. 1. The most significant result is that all the data for a given rock type collapse to approximately the same curve, regardless of the size of the wearflat or the diameter of the cutter compact. This suggests two important conclusions:

(1) The penetrating force on a worn cutter for a given depth of cut is directly proportional to the wearflat area. This implies that for a given rock and set of operating conditions the values of C_1 and n1 can be determined with a cutter having any measureable wearflat, and those parameters should also be valid for other stages of measureable wear.

(2) For a given depth of cut and a given wearflat area, a large worn cutter requires no greater penetrating force than a small cutter, yet the large cutter does remove more rock. This suggests an improved cutting efficiency with increased cutter size, at least within the range of

sizes considered.

Penetrating forces measured with sharp cutters in dry, non-interacting cuts are shown in Fig. 5. These data indicate another interesting result: the larger cutter requires no larger penetrating force than the smaller cutter, even in the sharp condition. In the tests with Berea sandstone at 0.08 inch, the larger cutter actually required slightly lower penetrating forces than the smaller cutter. Correlations of the form given by Eq. 2 were determined, and the resulting values of C_2 and n2 are shown in Fig. 5.

The cutter drag forces, F_d, measured in the dry, non-interacting cuts with worn cutters are shown in Fig. 6, plotted as a ratio with the penetrating force, F. We define this ratio as the cutter drag coefficient,

$$\mu_d = F_d/F \quad . \tag{3}$$

As in the previous work with a more limited range in wearflat area [3], we see that the worn cutter drag coefficient is a function of the rock type but is relatively independent of depth of cut and wearflat area. If a model is available to predict F, it is then possible to estimate F_d:

$$F_d = \mu_d F \quad , \tag{4}$$

where, for instance, $\mu_d \approx 0.65$ for worn cutters in Sierra White granite and $\mu_d \approx 0.95$ in Berea sandstone.

Drag coefficients for sharp cutters are shown in Fig. 7. When compared with the results for worn cutters, as represented by the curves, it is seen that sharp cutters have consistently higher drag coefficients. The larger cutter has slightly higher drag coefficients than the smaller cutter with deep cuts in both sharp and worn conditions.

Non-Interacting Cuts with Jet Assistance

Shown in Fig. 8 are the penetrating stresses measured with waterjets impinging on the rock surface ahead of the cutter. Note that the stresses obtained with 80 psi jets are similar to those measured in the dry cuts, as represented by the upper curve. The jet velocity with this low nozzle pressure is not sufficient to affect penetrating stresses, and the simple presence of water at the cutter/rock interface also seems to have little effect. At elevated nozzle pressures, however, penetrating stresses are significantly reduced. With jet pressures of 2000 psi, the penetrating stresses required to cut Sierra White granite to a given depth are reduced by 10 to 15%. With assistance from 4500 psi waterjets, cutter penetrating stresses are reduced by 50 to 65%.

Passes made over the rock surface without actual contact between the cutter and the rock revealed that the 2000 psi jet alone did not cause visible damage to the rock surface. The observed reductions in penetrating stresses in this case are probably due to improved cleaning at the cutter/rock interface. Efficient removal of cutting fines should help maintain greater stress concentration in the rock at the cutting edge.

At 4500 psi, the jet caused considerable damage to the rock surface, even though the nozzle standoff distance was greater than 1.5 inches. Though not a continuous cut, the path left by the jet in the granite resembled a series of closely-spaced irregular holes, some of which were up to

0.08 inch deep. The assistance given to the cutter by the jet in this case was due in large part to a reduction in the cutter cross-sectional area of cut and in the strength of the remaining rock surface.

The drag coefficients measured in the jet-assisted, non-interacting cuts are shown in Fig. 9, where they are compared with the results for the dry cuts. The drag forces are seen to be reduced by the presence of water, but they are not greatly affected by jet pressure. This suggests that the reduction in drag coefficient is caused simply by the lubrication effect of water, which reduces the friction component of the drag force. This supports a model for the drag force which considers the force to be the sum of two components [2]:

$$F_d = F_c + F_f \ , \qquad (5)$$

where F_c is the cutting force and F_f is the friction force. We may divide Eq. 5 by F and recognize that the friction coefficient, μ , is defined as the ratio F_f/F. The result is then

$$\mu_d = F_c/F_d + \mu \ . \qquad (6)$$

We thus see that a reduction in friction coefficient results in an equal reduction in drag coefficient. Measured friction coefficients between PDC cutters and Sierra White granite are 0.16 under dry cutting conditions and 0.07 when cutting with low-pressure waterjets directed at the cutter/rock interface [18]. The difference in friction coefficient of about 0.10 between the wet and dry cutting conditions is apparently translated to a comparable difference in drag coefficient between the two conditions, as predicted by Eq. 6 and confirmed in Fig. 9.

Other Observations

Considerable scatter exists in the data of Figs. 4-9. Since these tests were conducted under carefully controlled and monitored conditions, it is reasonable to assume that the scatter is inherent to the rock cutting process itself. For this reason, tests were generally conducted at least five times at each depth of cut in order to determine mean values of the cutter forces.

The laboratory-worn wearflats created against Sierra White granite were found to differ significantly from the field-worn wearflats. With the field-worn wearflats, the diamond portion of the wearflat was found to have worn parallel to the cutting direction. The WC/Co portion of the wearflats, however, was generally inclined at angles of 5-10° with respect to the cutting direction, as shown in Fig. 10. The length of the wearflat in contact with the rock, as measured with the carbon paper technique, ranged from 0.05 to 0.09 inch and was approximately constant over its width. These lengths were thus only two to four times the thickness (0.025 in) of the diamond layer on the compact. It is likely that these cutters were worn in relatively soft formations. The relative wear resistance of PDC and WC/Co apparently dominated the wear process. The WC/Co wore at a higher rate, thereby tending to keep only the diamond and a small portion of the WC/Co in contact with the rock. It is probable that the WC/Co wear is attributable mostly to contact with ground rock particles passing beneath the angled wearflat.

The laboratory-worn wearflats, on the other

hand, wore very nearly parallel to the cutting direction (within 1°). Field-worn cutters worn further in the laboratory against granite exhibited the same behavior. This indicates perhaps that the greater impact loading associated with hard-rock drilling, particularly in quartz-rich rock, tends to fracture off any PDC layers that are not fully supported by the WC/Co backup material. This tends to keep more of the WC/Co in contact with the rock, creating a duller condition. This wear mechanism could be a major contributor to poor drag bit life in hard or fractured rock.

DEVELOPMENT OF THE PDC BIT DESIGN CODE PDCWEAR

In this section, a theory for predicting cutter interaction is developed and incorporated into a general computer code for PDC bit design. Models used in the code for predicting cutter temperatures and wear rates are also developed and discussed.

Cutter Interaction Theory

Shown in Fig. 11 is a typical cutting pattern for a cutter on the leading face of a PDC bit. This cutting pattern imposes a given penetrating and drag force on the cutter, depending on the type of rock, the wearflat area, and the cutting conditions. It is postulated that there exists an equivalent non-interacting cut that would impose the same forces on the cutter as the actual rock surface profile seen in Fig. 11. The profile of the flat rock surface in this equivalent cut is represented as the heavy dashed line in the figure. The location of the equivalent flat surface relative to the bottom of the cut is δ_e, the effective depth of the equivalent non-interacting cut. By definition, the penetrating stress and force of the equivalent cut are equal to the penetrating stress and force, respectively, of the actual cut. Since the equivalent cut is also the same as a non-interacting cut, the effective depth of cut is then related to the actual penetrating stress:

$$F/A_w = C_1(\delta_e)^{n1} , \qquad (7)$$

or, alternatively, to the actual penetrating force:

$$F = C_2(\delta_e)^{n2} . \qquad (8)$$

Inspection of the figure shows that the location of the equivalent flat surface would probably be at a location between the high and low points on the actual rock cutting profile, as shown. A simple estimate of δ_e would then be the mean height of the actual profile:

$$\delta_e \cong \frac{1}{w_c}\int \Delta(x)\, dx . \qquad (9)$$

Since $\Delta(x)$ can be determined from geometry considerations, as shown below, it is possible to estimate δ_e and thereby predict cutter penetrating forces according to Eqs. 7 and 8.

This approach was tested in our previous work by measuring single-cutter forces during interacting cuts, as illustrated in Fig. 12. In these tests, a wide range in cutter interaction and thus δ_e was obtained by varying the lateral distance, d, to adjacent cuts. The results are presented in Fig. 13. The constants in the equations used for predicting the interacting

penetrating stresses were obtained from non-interacting test cuts as in the present study. The agreement seen here between measured and predicted penetrating stresses suggests that the approach can be used to estimate cutter performance under arbitrary interaction conditions.

Extending this approach to cutters placed at any location on a bit body requires the assumption that the size and shape, but not the orientation, of the cross-sectional area of cut controls the penetrating stress that develops during cutting. Shown in Fig. 14 is a cutter mounted on an arbitrary surface of the bit body. The cutter is mounted at an inclination angle, ϕ_c, with respect to the longitudinal (z') axis of the bit. Because of cutter interaction, the cross-sectional area of rock removed by this cutter is not necessarily symmetric about the cutter's longitudinal axis. In this case, the penetrating force develops a side component with respect to the longitudinal axis of the cutter.

Consistent with the case of the cutter on the leading face of the bit (Fig. 11), the equivalent flat cutting surface in this general case is inclined at the same angle as the overall slope of the actual rock cutting surface. The cutter wearflat is assumed to develop parallel to the equivalent surface and is therefore also inclined at the angle

$$\phi_w = \tan^{-1}\left[\frac{z_{c1} - z_{c2}}{x_{c2} - x_{c1}}\right] , \qquad (10)$$

where (x_{c1},z_{c1}) and (x_{c2},z_{c2}) are the first and last points of contact between the cutter and the rock, proceeding in the +x-direction. We define the angle ϕ_w as the radial wear angle.

The penetrating force develops normal to the equivalent flat cutting surface and is thus inclined at the radial wear angle with respect to the longitudinal axis of the bit. The effective depth of cut is also measured in this direction. Use of Eq. 9 to compute δ_e requires mathematical descriptions of the cut profiles for each cutter on the face of the bit under consideration. Shown in Fig. 15 is a reproduction of Fig. 14 with more pertinent parameters identified. The geometry of the cutter wearflat as it affects the cut profile is defined by the radial wear angle ϕ_w (Eq. 10) and the width of the wearflat, w (assumed known). The coordinates (x_{w1},z_{w1}) and (x_{w2},z_{w2}) define the intersections of the wearflat with the sharp segments of the cutting edge. As shown in Appendix A, these coordinates are given by the equations,

$$x_{w1} = R + (x_{w1})'_o \cos\phi_c + (z_{w1})'_o \cos\beta \sin\phi_c \qquad (11a)$$

$$z_{w1} = H - (x_{w1})'_o \sin\phi_c + (z_{w1})'_o \cos\beta \cos\phi_c \qquad (11b)$$

$$x_{w2} = R + (x_{w2})'_o \cos\phi_c + (z_{w2})'_o \cos\beta \sin\phi_c \qquad (11c)$$

$$z_{w2} = H - (x_{w2})'_o \sin\phi_c + (z_{w2})'_o \cos\beta \cos\phi_c , \qquad (11d)$$

where

$$(x_{w1})'_o = r_w \sin(\phi_w)'_o - \frac{w}{2}\cos(\phi_w)'_o \qquad (11e)$$

$$(z_{w1})'_o = r_w \cos(\phi_w)'_o + \frac{w}{2}\sin(\phi_w)'_o \qquad (11f)$$

$$(x_{w2})'_o = r_w \sin(\phi_w)'_o + \frac{w}{2}\cos(\phi_w)'_o \qquad (11g)$$

$$(z_{w2})'_o = r_w \cos (\phi_w)'_o - \frac{w}{2} \sin (\phi_w)'_o \qquad (11h)$$

$$r_w = \sqrt{r^2 - (\frac{w}{2})^2} \qquad (11i)$$

$$(\phi_w)'_o = \tan^{-1} [\tan(\phi_w)_o / \cos \beta] \qquad (11j)$$

$$(\phi_w)_o = \phi_w - \phi_c \qquad (11k)$$

and H is given by Eq. A-9 in Appendix A. The cutting profile of the cutter can now be determined. For values of x such that

$$x_{w1} < x < x_{w2} \quad , \qquad (12)$$

the cutting profile is that of the cutter wearflat, and the z-coordinate is given by the straight-line equation

$$z = z_{w1} + \left[\frac{x - x_{w1}}{x_{w2} - x_{w1}}\right] (z_{w2} - z_{w1}) . \qquad (13)$$

For values of x outside this range, the cutting profile is described by the equation for an ellispse [19]:

$$z = C_3 [D(x - R) \pm \sqrt{E - (x - R)^2}] + H \qquad (14a)$$

$$y = 0 \qquad (14b)$$

$$C_3 = \frac{rb}{E} \qquad (14c)$$

$$D = -\sin \phi_c \cos \phi_c (r^2 - b^2)/rb \qquad (14d)$$

$$E = r^2 \cos^2 \phi_c + b^2 \sin^2 \phi_c \qquad (14e)$$

$$b = r \cos \beta \qquad (14f)$$

A computer program that implements the above equations has been written and is called PDCWEAR. The algorithm used in this program is illustrated in Fig. 16. It is an extension of an algorithm used in previous work [19]. During one revolution of the bit, each cutter passes through a radial plane containing the x- and z-axes of the hole coordinate system. The x-axis is divided into a number of equal-sized elements of length Δx. At each value of x corresponding to the midpoint of these elements, a procedure determines which cutters interact at that cutting radius by comparing x with the dimensional limits of each cutter. For each of these cutters, the program checks to determine whether the cutting edge at that location is sharp or is part of the wearflat. For values of x within the range given by Eq. 12, the wearflat coordinate equation, Eq. 13, is used to determine z_k, the z-coordinate of the kth cutter encountered at that radial position x. If x is not within this range for a given interacting cutter, Eq. 14 is used to determine the z-coordinate of that cutting profile. In either case, the incremental cross-sectional areas of cut,

$$\Delta A_r = \Delta x (z_k - z_{k-1}) \quad , \qquad (15)$$

are assigned to the appropriate cutters, depending on the angular location of the cutters on the bit face. The incremental volumes of cut,

$$\Delta V_r = 2\pi x (\Delta A_r) \quad , \qquad (16)$$

are assigned to the same respective cutters.

The effective depth of cut must be computed in a direction perpendicular to the cutter wearflat. The equivalent bottom of each cut is described by the line

$$z_b = z_{bc} + (x_{bc} - x) \tan \phi_w \,, \qquad (17a)$$

where $z_{bc} = H - (x_{bc})_o \sin \phi_c + (z_{bc})_o \cos \phi_c$ (17b)

$$x_{bc} = R + (x_{bc})_o \cos \phi_c + (z_{bc})_o \sin \phi_c \qquad (17c)$$

$$(x_{bc})_o = r_w \sin (\phi_w)'_o \qquad (17d)$$

$$(z_{bc})_o = [r_w \cos (\phi_w)'_o] \cos \beta \,. \qquad (17e)$$

At each point x, the z-location of the bottom of the kth cut, $(z_b)_k$, is given by Eq. 17. The effective depth of cut for the kth cutter is then

$$\delta_e = \frac{1}{n_x} \sum_{i=1}^{n_x} \Delta_i \,, \qquad (18a)$$

where $\Delta_i = [(z_b)_k - (z)_{k-1}] \cos \phi_w$ (18b)

and n_x is the number of Δx elements over which a given cutter interacts with the rock formation.

Forces and Moments Acting on the Bit

Once the effective depths of cut are computed, the cutter penetrating force can be estimated using Eq. 8 for sharp cutters and Eq. 7 for worn ones. The algorithm actually used in PDCWEAR computes penetrating forces based on both equations and uses the larger of the two computed values. This logic is based on the fact that Eq. 7 becomes invalid as A_w tends to zero. Since the lowest penetrating force possible is the one obtained with a sharp cutter, it is evident that Eq. 8 is more accurate than Eq. 7 in cases where Eq. 7 predicts lower forces.

As seen in a previous section, the cutter correlation constants C_1, n1, C_2, and n2 can be significantly affected by waterjet assistance. The effects of other factors that control inherent drillability, such as backrake angle, are also contained within the values used for these parameters . As a result, PDCWEAR is written so that two different types of cutters (A and B) can be specified, each with its own set of correlation constants. In this way, the effects of different design options, such as providing jet assistance to selected cutters on a bit face, can be assessed.

After the penetrating force is computed using the appropriate correlation constants, it may be resolved into radial and longitudinal (vertical) components in the bit coordinate system:

$$F_r = -F \sin \phi_w \qquad (19)$$

and

$$F_v = -F \cos \phi_w \,. \qquad (20)$$

The drag force on each cutter is estimated using Eq. 4. This force is directed opposite to the direction of the cutter velocity vector. In terms of the bit coordinate system, each drag force is a purely circumferential force about the longitudinal axis. (See Fig. 17.)

The resultant bit forces and moments arising from the cutter forces can now be determined. The total weight on bit (WOB) is simply the sum of the longitudinal components:

$$WOB = \sum_{j=1}^{n_c} (-F_v)_j \quad , \tag{21}$$

where n_c is the number of cutters on the bit. The drilling torque is the sum of the moments caused by the circumferential drag forces:

$$T = \sum_{j=1}^{n_c} (F_d)_j (x_{bc})_j \quad . \tag{22}$$

Unless the cutters are placed such that the cutting forces balance each other, there will be a net side force acting on the bit. The component of the side force in the x'-direction is

$$F'_x = \sum_{j=1}^{n_c} [(F_r)_j \cos(\theta)_j + (F_d)_j \sin(\theta)_j] \quad . \tag{23}$$

Likewise, in the y'-direction,

$$F'_y = \sum_{j=1}^{n_c} [(F_r)_j \sin(\theta)_j - (F_d)_j \cos(\theta)_j] \quad , \tag{24}$$

giving a resultant side force of

$$F_s = \sqrt{(F'_x)^2 + (F'_y)^2} \quad . \tag{25}$$

A different mode of bit imbalance is the net bending moment about the x' and y' axes:

$$M'_x = \sum_{j=1}^{n_c} [-(F_r)_j \sin(\theta)_j (z'_{bc})_j + (F_v)_j (x_{bc})_j \sin(\theta)_j + (F_d)_j \cos(\theta)_j (z'_{bc})_j] \tag{26}$$

$$M'_y = \sum_{j=1}^{n_c} [(F_r)_j \cos(\theta)_j (z'_{bc})_j - (F_v)_j (x_{bc})_j \cos(\theta)_j + (F_d)_j \sin(\theta)_j (z'_{bc})_j], \tag{27}$$

where $$z'_{bc} = z_{bc} - f_r (360 - \theta)/360 \tag{28}$$

and f_r is the feed rate of the bit (penetration/revolution), defined in Eq. A-10 of Appendix A. The resultant bending moment is simply the vector sum of the x and y components:

$$M = \sqrt{(M'_x)^2 + (M'_y)^2} \quad . \tag{29}$$

Cutter Wearflat Temperatures

The cutter temperatures are calculated using an equation developed in our earlier work [1,4,5]:

$$\bar{T}_w = T_f + \frac{\mu F V f}{A_w} \left[1 + \frac{3\sqrt{\pi}}{4} f k_2 \left(\frac{V}{L x_2}\right)^{1/2}\right]^{-1} \quad . \tag{30}$$

The cutting speed of each cutter is dependent on the rotary speed, N, of the bit and the radial location of the wearflat, x_{bc}:

$$V = 2\pi N x_{bc} \quad . \qquad (31)$$

The thermal response function, f, is defined in our earlier work as the temperature rise of the cutter wearflat per unit frictional heat flowing into the cutter. The numerical value of f depends on the geometry of the cutter, material properties of the cutter, and the cutter cooling coefficient. Values of f computed with finite element thermal models of stud-mounted, 0.5-inch diameter compact cutters are reported in Refs. 1, 4, and 5. New results obtained with larger 0.75-inch diameter compact cutters are reported in Ref. 14. These results indicate that larger cutters run slightly hotter than smaller ones. Results for both cutter sizes are tabulated and used in PDCWEAR.

Cutter Wear Rates

To prevent thermally-accelerated wear, which is one to two orders of magnitude more rapid than ordinary abrasive wear, wearflat temperatures must be kept below 350°C. For temperatures below this critical value, a simple model developed in our earlier work [3] concludes that the volume of cutter material, V_w, worn away per unit length of hole drilled, ℓ_h, is related to several design and operating parameters:

$$\frac{dV_w}{d\ell_h} = \frac{2\pi F x_{bc} C_6 N}{ROP} \quad , \qquad (32)$$

where the constant C_6 is defined as the abrasive wear constant and is a function of the abrasiveness of the rock and the abrasion-resistance of the drag cutter materials. We may define a wear ratio (WR) that describes the volumetric wear rate of each cutter relative to that of a reference cutter. We take this reference to be cutter 1, nearest the center of the bit. Thus

$$WR = \frac{(dV_w/d\ell_h)}{(dV_w/d\ell_h)_1} = \frac{Fx_{bc}}{(Fx_{bc})_1} \quad . \qquad (33)$$

This quantity provides a measure of wear uniformity among cutters independent of the abrasive wear constant C_6.

The existence of a wear ratio also suggests the possibility of estimating relative cutter wear and modifying cutter geometries to determine the effects of wear on bit performance. As a bit drills a distance $\Delta\ell_h$ from point 1 to point 2, the volume of material worn from the cutter changes from $(V_w)_1$ to $(V_w)_2$, where

$$(V_w)_2 = (V_w)_1 + \frac{dV_w}{d\ell_h} \Delta\ell_h \quad , \qquad (34)$$

if $dV_w/d\ell_h$ is relatively constant over the drilling distance. We may then divide Eq. 34 by the same equation evaluated for a reference cutter (r) and define

$$\Delta V_w = (V_w)_2 - (V_w)_1 \qquad (35)$$

to get

$$\frac{\Delta V_w}{(\Delta V_w)_r} = \frac{dV_w/d\ell_h}{(dV_w/d\ell_h)_r} \quad , \qquad (36)$$

or, using Eq. 33,

$$\Delta V_w = \frac{WR}{(WR)_r} (\Delta V_w)_r \quad . \qquad (37)$$

Thus, if we specify the change in the wear volume for the reference cutter, $(\Delta V_w)_r$, the wear volumes of the other cutters can also be determined using the computed wear ratios. If the value of the abrasive wear constant C_6 is known for the rock of interest, the distance $\Delta \ell_h$ drilled in wearing away the volume $(\Delta V_w)_r$ can be determined. Combining Eqs. 32 and 34, we obtain the result

$$\Delta \ell_h = \frac{(\Delta V_w)_r \ ROP}{2\pi \ (Fx_{bc})_r \ C_6 N} \quad . \tag{38}$$

It is more convenient to express cutter wear in terms of dimensions that can be readily measured. It is, therefore, necessary to determine the relationships between cutter wear volume and the other wearflat dimensions. These relationships are functions of the wear mode. As discussed previously, two distinct wear modes seem to occur. In hard, brittle rock, the wearflat tends to develop parallel to the cutting direction. In our previous work, we showed that the length of such a wearflat may be expressed as a simple function of the wear volume [3]:

$$L = C_4 \ V_w^{n4} \quad , \tag{39}$$

or, alternatively, as a function of the wearflat area [1]:

$$L = C_5 \ A_w^{n5} \quad , \tag{40}$$

where C_4, n4, C_5, and n5 are functions of the cutter compact radius and backrake angle. Values of these parameters have been determined for 20° backrake cutters with 0.5-inch and 0.75-inch diameter compacts, as listed in Table II. This analysis assumes that the wearflat is in the center of the cutting profile, i.e. $\phi_w = \phi_c$, but the error for cutter side wear is not large with the backrake angles generally used in PDC bit design (<30°). The width of the wearflat, measured at the diamond face, is

$$w = 2\sqrt{r^2 - (r - L \sin \beta)^2} \quad . \tag{41}$$

For the hard-rock wear mode, we may now specify a new wearflat area for the reference cutter, compute the associated new wear volume using Eqs. 39 and 40 and compare this with the old wear volume to determine $(\Delta V_w)_r$. Eqs. 35 and 37 can then be used to compute the new wear volume, $(V_w)_2$, for every other cutter on the bit. From these volumes, the new wearflat length, area, and width for each cutter can calculated using Eqs. 39-41. Re-running the program with the new wear configuration then allows the user to assess the effects of the predicted wear pattern on bit performance.

In the soft-rock wear mode, the PDC layer wears parallel to the cutting direction, but the WC/Co portion of the wearflat develops at an angle, as previously discussed. Although this angle prevents most of the WC/Co from directly contacting the rock surface, the angle is sufficiently small that Eqs. 39 and 40 are still approximately true, provided we consider the quantities to represent quantities related to the total (t) wearflat comprised of both PDC and WC/Co. Thus

$$L_t \cong C_4 \ (V_w)_t^{n4} \tag{42}$$

and

$$L_t \cong C_5 \ (A_w)_t^{n5} \quad . \tag{43}$$

The width of the wearflat at the diamond face is then

$$w \approx 2\sqrt{r^2 - (r - L_t \sin \beta)^2} . \qquad (44)$$

The length of the wearflat in contact with the rock, L, is assumed in this wear mode to be constant at 0.07 inch, the mean value measured with the field-worn cutters in the experiments previously described. The model for the soft-rock wear mode then assumes that the wearflat area in contact with the rock grows by increasing the width, w, over which the wearflat exists; thus

$$A_w \cong Lw . \qquad (45)$$

The procedure for this wear mode is to specify a new wearflat area A_w for the reference cutter, compute the new wear volume $(V_w)_t$ for that cutter using Eqs. 42-45 and compare this with the current wear volume to determine $(\Delta V_w)_r$. Eqs. 35 and 37 are used to determine the new wear volumes for all other cutters, and Eqs. 42-45 are then used to determine the new wearflat areas, lengths, and widths for each cutter in the advanced wear state.

A loop is written in the program to allow the user to repeat the wear process described above as many times as desired. The user can run the program for several different bit wear states ranging from sharp to severely worn. This provides a means for obtaining predicted results necessary for assessing drilling performance over the life of the bit.

DEMONSTRATION OF THE COMPUTER PROGRAM

In this section, the program PDCWEAR is demonstrated by analyzing the baseline bit design shown in Fig. 18. This is an 8-1/2 inch PDC bit utilizing 21 cutters with 0.75 inch diameter compacts mounted on 1.0 inch diameter studs. The parameters that describe the location and orientation of the center of each cutter compact on the bit face are listed in Table III. In general, the cutters are arranged in a three-arm spiral pattern.

Operating conditions used in the baseline analysis are listed in Table IV. The single-cutter data that are used are those obtained with the test cuts made in Sierra White granite (Figs. 4-9). The rock properties used are also those of granite, with the exception of the abrasive wear constant, C_6. Data on this parameter were not available for Sierra White granite. Data were available for Jack Fork and Nugget sandstones, however, and these indicate that with wearflat temperatures below 350°C, the abrasive wear constant has a value on the order of that listed in the table. Although both of these sandstones are relatively hard and abrasive, it is unlikely that they are as abrasive as Sierra White granite.

A rotary speed of 100 RPM and a cooling fluid temperature of 80°F were assumed in the baseline analysis in order to match laboratory drilling conditions. Penetration rates of of 10-50 ft/hr were specified.

The cutters were initially assumed to be sharp, and the cutter and bit performance parameters were computed. The cutting profiles were then allowed to change according to the computed wear ratios and a specified new wearflat area for the cutter with the highest wear rate.

The hard-rock wear mode was chosen for the baseline analysis. Performance parameters were computed for the new configuration, and the process was repeated. Since the wear ratio is a function of the wear configuration, small (0.005 in^2) increments in wearflat area growth were specified. Wear ratio is also a function of penetration rate; the ratios used to compute cumulative wear were those computed at 30 ft/hr. The cutters were allowed to wear until the performance parameters indicated that the bit was "worn out."

With the baseline bit design, cutter 15 wore at a higher rate than any other cutter. The growth of this cutter's wearflat area is plotted in Fig. 19 as a function of the computed footage drilled by the bit. We designate three points along this curve as reference wear conditions for the bit: "sharp" when all cutter wearflat areas are zero; "worn" when the reference cutter wearflat area is 0.04 in^2; and "worn out" when the reference cutter wearflat area is 0.100 in^2. The results indicate that the bit will drill 460 ft before reaching the designated "worn" stage, and it will drill 975 ft before it is worn out.

The distribution of cutter wear in each of the designated stages of bit wear is shown in Fig. 20. Note that with this design, cutters near but not on gage tend to experience the greatest wear (cutters 13-16). The gage cutters (19-21) wear slightly less than those on the leading face of the bit (4-6).

Baseline cutter and bit performance parameters in each of the bit wear stages are plotted in Figs. 21-27. In Fig. 21, the predicted penetrating forces are shown. When the bit is sharp, the penetrating forces tend to decrease from the center of the bit out toward gage. This is caused by increased cutter interaction resulting from closer radial spacing of cutters near gage. As the cutters wear, however, the overriding effects of wearflat area cause the penetrating force distribution to change. The wear ratios resulting from the computed penetrating forces are shown in Fig. 22. The integrated effects of the wear ratios at all stages of wear are responsible for the wearflats areas shown in Fig. 20.

The computed wearflat temperatures for the baseline analysis are shown in Fig. 23. These results indicate that, even when the cutters are severely worn, temperatures are below 350°C, and thermally-accelerated wear should not occur. It should be noted, however, that the friction coefficient assumed for this analysis was only 0.07, and the cooling fluid temperature was assumed to be only 80°F. If either of these quantities were higher, which is likely under actual drilling conditions, cutter wearflat temperatures could exceed the critical level, and accelerated wear would occur.

The computed WOB is plotted as a function of ROP in Fig. 24. We see a large effect of cutter wear on bit performance. Although the bit requires only 3500 lbf WOB to drill at 30 ft/hr when sharp, it requires nearly ten times that weight to maintain the same ROP when the bit is worn out.

Perhaps a more compelling indication that the bit is worn out is the excessive drilling torque predicted for this wear condition. As shown in Fig. 25, torque increases with cutter wear to levels that conventional drilling practices would probably not tolerate, resulting in the bit being pulled.

The net side force predicted for the baseline analysis is shown in Fig. 26. This force would develop if the bit were constrained by the walls of the borehole to follow a straight line and to rotate concentrically about its geometric center. In reality, a bit side force would tend to make the bit cut deeper on the side opposite the force, resulting in an oversize hole and eccentric rotation of the bit, or bit wobble. Such imbalance in the bit design is usually undesirable. When worn, the side forces are less than 3% of the WOB. This would seem to suggest that the bit is not greatly unbalanced in the worn condition, but it is not known what levels of side force are significant, especially under dynamic conditions.

Similar comments can be made with respect to the predicted bending moments, shown in Fig. 27. In this case the drill pipe is capable of providing a reactive torque to prevent excessive tilting of the bit. Again, however, the effects of the bending moment on the dynamic response of the drill string are not known but could be significant.

Now that the baseline results have been established, the effects of several important design and operating variables can be assessed. These effects are determined by modifying the bit design and/or operating parameters and repeating the analysis. Results are illustrated by comparing the performance parameters predicted after drilling the same footage as in the baseline analysis (i.e., 0, 460, and 975 ft).

Effects of Bit Profile

Perhaps the most obvious of the bit design variables is the bit profile. The profile used in the baseline analysis was relatively flat, with only a 1.0 inch range in cutter longitudinal locations over the 8.5-inch diameter bit. To assess the effects of bit profile, an analysis was perfomed using the bullet-nose bit design shown in Fig. 28. The cutter locations are identical to those of the baseline analysis, except that the longitudinal locations range over 4.0 inches instead of 1.0 inch, and there is no concave portion in the center of the bit.

Shown in Fig. 29 are the predicted wearflat areas for the bullet-nose bit. The primary effect of bit profile in this example is to increase wear on most of the cutters, especially those near the nose of the bit (cutters 1-9). This result agrees with field experience, which generally shows that flatter bit profiles are necessary when drilling hard rock, where wear is usually a problem.

Although the wearflats grow faster with the bullet-nose bit, the computed results indicate that the WOB is, in the early stages of drilling, actually lower than that of the baseline analysis, as shown in Fig. 30. When plotted in this manner, it is seen that for a given WOB, the bullet-nose bit drills at a much higher ROP than the baseline bit after both have drilled 460 ft of hole. Since the bullet-nose bit wears faster, however, the effects of wearflat area eventually become dominant. By the time the bullet-nose bit has drilled 950 ft, it requires the same WOB that the baseline bit required when it was declared worn out at 975 ft. The last 25 ft of drilling are accompanied by a rapid increase in WOB requirements for the bullet-nose bit.

The predicted drilling torque for the bullet-nose bit was higher that that for the baseline analysis. In the sharp condition, the differences

ranged from 8 to 25%, depending on ROP. After 460 ft of drilling, the bullet-nose bit torque was 12 to 17% higher, and after 975 ft, it was 8 to 25% higher. Side forces and bending moments were also more excessive with the bullet-nose bit.

Effects of Cutter Placement Density

The number of cutters used in this analysis was reduced from that of the baseline analysis, from 21 to 15, in order to assess the effects of using a lower cutter placement density. Cutters 8, 10, 12, 14, 16, and 18 were removed from the baseline design, with other cutters remaining in their oringinal positions. The cutters that were removed were so chosen in an effort to maintain balance in the design.

In this case, the remaining cutters in the reduced density region (cutters 7-19) experienced greatly increased wear, as shown in Fig. 31. This is caused by the reduced interaction and, consequently, higher penetrating forces on these cutters. The predicted wearflat cutter temperatures at a ROP of 30 ft/hr indicate that cutter 15 exceeds 350°C after a hole length of 880 ft; thus the cutter 15 wearflat area would be even larger than that shown at 975 ft.

Although the number of cutters used in the two bits were significantly different, the difference in required WOB was relatively small. When the bits are sharp, the 15-cutter bit requires 4 to 7% more WOB. After 475 ft of hole, the 15-cutter WOB is lower by 4 to 8%. By the time both bits have drilled 975 ft, the 15-cutter WOB is 3 to 11% lower. Of course, if the accelerated wear of the cutters that experience thermal wear were taken into account, the larger wearflat areas for those cutters would have increased the WOB significantly with further drilling after 880 ft. Furthermore, since wear rates increase by 1 to 2 orders of magnitude during this mode of wear, the affected cutters can, for all practical purposes, be considered destroyed. When this happens, the bit may be left in a configuration that will not drill.

These results suggest two ways for defining bit life that may be related. The first is the drilled footage at which thermally-accelerated wear begins on any cutter. In this case, the life of the 15-cutter bit would be 880 ft, and that of the baseline bit would be 1220 ft.

Alternatively, we may define the bit life as the drilled footage at which a performance parameter, such as WOB, drilling torque, or bit imbalance, reaches some selected level. In the baseline analysis, we arbitrarily selected a WOB of 40,000 lbf (at 50 ft/hr) as a limit on bit life, based on practical levels for this size bit. This resulted in the WOB-bit life criterion of 33,000 lbf at 30 ft/hr in the baseline analysis. If thermally-accelerated wear occurs, as with the 15-cutter bit, the resulting rapid growth in WOB would cause the bit to more rapidly reach the limit defining bit life. Thus, if the temperature-bit life criterion is reached, it is probable that any practical WOB-bit life criterion will be reached soon after.

In addition to changing the number of cutters, placement density can be modified locally by moving cutters radially and circumferentially. The radial placement of cutters is one of the most important parameters in bit design. To achieve more uniform wear, cutters can be shifted radially to provide a higher placement density in regions of excessive

wear and lower density in regions of low wear.

The circumferential placement of cutters is important because it affects bit balance during drilling. Excessive side forces can be reduced by shifting cutters circumferentially in the proper directions. Circumferential placement also affects cutter forces because it determines how the feed rate of the bit bit is distributed among the cutters (see Eq. A-9 of Appendix A).

Effects of Bit Rotary Speed

For a given penetration rate, the feed rate of the bit (penetration/revolution) decreases as the bit rotary speed is increased (Eq. A-10). This implies that for a given wear configuration, a selected ROP can be achieved with a lower WOB by increasing rotary speed. To investigate this effect, an analysis was performed by changing the rotary speed in the baseline analysis from 100 to 200 RPM.

The results indicate that when the bit is sharp, the higher rotary speed does indeed reduce the WOB requirements,by 42 to 54%. Similar reductions in drilling torque were predicted at the higher speed. The lower bit feed rate, however, causes each cutter to travel twice as far in drilling the same length of hole. As a result, the cutters wear faster with respect to footage drilled. This effect is illustrated in Fig. 32. Note that all cutters experience increased wear at the higher rotary speed. The wear on cutters 11-18 after 975 ft of hole would be even greater than that shown, because the predicted wearflat temperatures for those cutters exceed 350°C after only 650 to 900 ft.

As a result of the computed wear pattern, the WOB for the higher rotary speed is 11 to 18% higher after 465 ft and 25 to 26% higher after 975 ft of hole. Similar increases in drilling torque were predicted for the higher speed. The conclusion we reach is that, even under conditions where thermal wear effects are not important, increased rotary speed is detrimental to bit life and, consequently, to the penetration performance of the bit. This agrees with results obtained in our earlier work [3]. Under conditions where a higher ROP is required, it is better to achieve it by increasing WOB rather than rotary speed.

Effects of Waterjet Assistance

In the baseline analysis, cutters 13-16 experienced greater wear than the other cutters. In this analysis, we demonstrate the beneficial effects of waterjet assistance by simulating placement of jets in front of those cutters. This is done by using, for these cutters, the single cutter correlation constants measured in the tests with 4500 psi waterjets (Fig. 8).

Shown in Fig. 33 are the computed wear distributions. Waterjet assistance is seen to reduce wear by more than one-half on the assisted cutters. Furthermore, since these cutters do not wear as fast as the surrounding ones, they remove more rock than they would otherwise remove in the advanced wear states. As a result, they interact more with the surrounding cutters, thereby reducing wear on those cutters as well. This effect is noticeable as far in toward the center of the bit as cutter 5.

The reduced wear on the bit is responsible for a significant improvement in drilling performance. The WOB required with the jet-assisted bit was

computed to be 19 to 23% lower after 460 ft of hole and 23 to 27% lower after 975 ft. Even greater reductions in drilling torque were predicted for the jet-assisted bit: 27 to 33% after 460 ft and 29 to 36% after 975 ft of drilling. If WOB is used as the criterion for declaring the bit worn out, the jet-assisted bit is predicted to have a bit life of 1225 ft, as compared with 975 ft in the baseline analysis. If the onset of thermally-accelerated wear is used as the bit life criterion, the jet-assisted bit drills for 1450 ft, compared with 1220 ft in the baseline analysis.

Effects of Wear Mode

In this analysis, the soft-rock wear mode was specified to demostrate the effects on wear patterns and bit performance. Results are shown in Fig. 34. After drilling 460 ft, the cutter wear pattern is quite similar to that computed for the baseline analysis. Beyond this footage, however, the two wear modes produce very different results. In the hard-rock wear mode, the wearflat area in contact with the rock is a strong fucntion of the volumetric wear, which in turn is proportional to penetrating force. Since the wearflat area has a large effect on penetrating force, wear in the hard-rock wear mode tends to occur at an accelerating rate with respect to footage drilled, even in the absense of thermal effects.

The wearflat area in the soft-rock wear mode, however, is not as sensitive to wear volume. In other words, a given increase in $dV_w/d\ell_h$ does not produce as large an increase in A_w as it does in the hard-rock wear mode. As a result, the wearflat area growth rate actually decreases as drilling continues. As a result, the predicted wearflat areas grow by only about 20% between hole lengths of 460 and 975 ft. This compares with 50 to 150% growth in the case of the hard-rock wear mode over the same footage.

The performance parameters in the soft-rock wear mode behave in a similar fashion. The WOB requirements after 460 ft of hole are within 4% of those predicted for the hard-rock wear mode. By the time both bits have drilled 975 ft, however, the bit worn in the soft-rock mode requires 49 to 50% less WOB than that in the hard-rock mode. Similar results were obtained with respect to drilling torque.

Because of the modest wearflat growth, the cutter temperatures in the soft-rock wear mode never approached the critical 350°C limit before the cutters were worn to the center of the compacts. When the wear reached this point, at 3370 ft, the calculations were terminated, and the bit was considered worn out. In terms of the WOB-bit life criterion of 33,000 lbf at 30 ft/hr, the bit never wore out. At 3370 ft, the WOB requirements at 30 ft/hr were only 18,700 lbf.

DISCUSSION

The computer code developed in this study predicts that the baseline bit design will drill relatively hard rock at a rate of 10-50 ft/hr and will last for approximately 1000 ft with a WOB of less than 40,000 lbf and a drilling torque of less than 6000 ft-lbf. These and other predicted results appear quite reasonable and are comparable to performance typically achieved with this size of bit.

For example, in geothermal drilling tests in the Imperial Valley, California, an 8-3/4" PDC bit drilled 555 ft at an average ROP of 55 ft/hr, with an estimated life of about 1000 ft [20]. The drilled interval contained sandstone, shale, siltstone, and igneous formations. The unconfined compressive strength of the sandstone in this interval was 11,000 psi, about one-half that of Sierra White granite, the cutting coefficients of which were used in the present analysis. Under the elevated downhole stresses present in the field test, however, the strength of the sandstone may be comparable to that of the granite at atmospheric pressures.

The thermal conditions assumed in the analysis were relatively mild. Downhole cooling fluid temperatures typically exceed 125°F in petroleum drilling and 200°F in geothermal drilling, well above the 80°F assumed in the analysis. Friction coefficients of 0.03-0.20 in water and 0.10-0.32 in air have been measured between PDC cutters and rock. It is therefore possible for the cutter wearflat temperatures to exceed those predicted in the baseline analysis, according to Eq. 30. In that case, thermal wear effects could reduce bit life well below the 1000 ft predicted here.

It has been shown that bit profile can significantly affect bit performance. This is due to the fact that the profile not only affects cutter density and thus interaction, but it also controls the orientation of the cutter penetrating forces. Forces oriented at steep angles, such as those on the side of the bullet-nose bit, contribute directly to cutter wear and bit side forces but have less relative impact on WOB. This explains how a bit design can drill with lower WOB but still experience more rapid wear than a different design.

Nozzles such as those used in the experimental part of this work would produce jets that flow at rates on the order of 12-18 gal/min with nozzle pressure drops of 2000-4500 psi. Since total drilling fluid flow rates of approximately 300 gal/min are typical for this size bit, it appears that up to 16-25 nozzles could be utilized on a single bit to assist PDC cutters. The resulting reduction in cutter forces could extend the applicability of PDC bits to much harder formations and more severe operating conditions. Limitations imposed by space requirements and the tendency for nozzles to plug would need to be overcome, but the potential benefits make the concept attractive.

Bit life in the soft-rock wear mode has been shown to be much greater than that in the hard-rock wear mode. This finding could explain the wide range in bit wear that is sometimes found in formations with apparently similar strengths. If the formation is fractured or has a high percentage of quartz, the probability that the cutters will wear in the hard-rock wear mode is increased, regardless of the apparent strength of the rock. The fact that some PDC bits have experienced bit life as long as 20,000 ft [21], however, is evidence that the soft-rock wear mode is operative under certain conditions.

Finally, it should be noted that many of the complex phenomena that contribute to PDC bit wear and performance are by no means completely understood. In this paper, we have developed and used simple models to describe various mechanisms so that the approach can be easily modified as more complete understanding becomes available. More

work needs to be done, for example, under elevated fluid and rock stresses to determine how downhole conditions affect these mechansims. In particular, the effects of ambient pressure on the benefits of waterjet assistance should be investigated. The approach as a whole needs to be tested by comparing predicted bit performance parameters, such a WOB and drilling torque, with results measured in full-scale PDC bit tests under carefully controlled atmospheric and elevated pressure conditions.

CONCLUSIONS

1) The penetrating force imposed on a worn PDC cutter at a given depth of cut is approximately proportional to the wearflat area in contact with the rock.

2) Within the limited range of cutter compact sizes tested (0.5-0.75 inch), the penetrating force is independent of compact diameter. This implies that larger cutters are more efficient in rock removal than smaller ones.

3) The penetrating stress required to cut to a given depth can be significantly reduced by directing low- to moderate-pressure waterjets onto the rock surface immediately ahead of the cutter. Reductions of 10-15% at 2000 psi nozzle pressure drop and 50-65% reductions at 4500 psi were measured in the present study, which was conducted at atmospheric pressures in granite.

4) Two distinct PDC cutter wear modes occur, depending on the type of rock drilled. Soft, plastic rocks tend to wear the flat at an angle with respect to the rock surface, which keeps a smaller area in contact with the rock and the cutter in a sharper condition. Hard, brittle rocks and conditions under which cutter impact loading is prevalent tend to wear the flat parallel to the rock surface, leading to a larger area in contact with the rock and higher cutting forces.

5) A method has been developed for using single-cutter data to predict cutter forces and bit performance for arbitrary PDC bit designs. This method has been shown to produce reasonable predictions of WOB, drilling torque, ROP, and bit life.

6) Unless cutter locations are carefully chosen, significant bit side forces and bending moments can develop during drilling. The resulting bit imbalance can cause bit wobble, leading to an overgage hole and possible bit deviation.

7) Bit profile can significantly affect PDC bit performance and wear. It has been shown that bits with sharper profiles tend to intitially require less WOB than flat profiles, but sharper profiles wear faster and eventually require greater WOB.

8) The distribution of cutters on a PDC bit can be used as a means for equalizing wear across the bit face. Cutters in regions of low placement density wear faster than those where placement density is high. Within limits, the WOB and torque required to drill at a specified penetration rate is relatively independent of the number of cutters used on the bit. A bit with fewer cutters will,

however, wear faster and eventually require greater WOB.

9) Increased bit rotary speed is detrimental to bit life, even under conditions where thermal wear effects are not important. Doubling the rotary speed from 100 to 200 RPM initally reduces the WOB required to drill at a specified rate, but more rapid wear occurs at the higher speed and eventually leads to greater WOB requirements and lower bit life.

10) Waterjet assistance can significantly increase bit life and reduce WOB and torque requirements. Greater than 20% improvements in bit life and 19-36% reductions in WOB and torque are predicted for a design utilizing only four nozzles operating at 4500 psi pressure drop. If space limitations and nozzle plugging problems could be resolved, this technique could be used to significantly extend the range of applicability of PDC bits.

NOMENCLATURE

A_r = cross-sectional area of rock removed by a cutter (in^2)
ΔA_r = incremental cross-sectional area of rock (in^2)
A_w = cutter wearflat area in contact with rock (in^2)
$(A_w)_t$ = total cutter wearflat area (in^2)
b = r cos ß (in)
C_1 = correlation constant in Eq. 1 (psi/in^{n1})
C_2 = correlation constant in Eq. 2 (lbf/in^{n2})
c_2 = rock specific heat (Btu/lbm°F)
C_3 = parameter defined in Eq. 14c
C_4 = constant in Eq. 37a (in^{1-3n4})
C_5 = constant in Eq. 37b (in^{1-2n4})
C_6 = abrasive wear constant (in^2/lbf)
D = parameter defined in Eq. 14d
E = parameter defined in Eq. 14e
f = thermal response function ($in^2hr°F/Btu$)
f_r = bit feed rate (in/rev)
F = cutter penetrating force (lbf)
F_c = cutting force, see Eq. 6 (lbf)
F_d = cutter drag force, see Eq. 6 (lbf)
F_f = cutter friction force, see Eq. 6 (lbf)
F_r = radial component of cutter penetrating force (lbf)
F_s = resultant side force on bit (lbf)
F_v = longitudinal (vertical) component of cutter penetrating force (lbf)
F'_x = bit side force in x' direction (lbf)
F'_y = bit side force in y' direction (lbf)
H = cutting height of cutter compact center (in)
H' = longitudinal position of cutter compact center on bit (in)
k_2 = thermal conductivity of rock (Btu/hr ft°F)
ℓ_h = length of hole drilled (ft)
L = length of cutter wearflat in contact with rock (in)
L_t = total length of cutter wearflat (in)
M = resultant bit bending moment (ft-lbf)
M'_x = bit bending moment about x'-axis (ft-lbf)
M'_y = bit bending moment about y'-axis (ft-lbf)
n_1 = correlation exponent in Eq. 1

n_2 = correlation exponent in Eq. 2
n_4 = exponent in Eq. 37a
n_5 = exponent in Eq. 37b
n_c = number of cutters on bit
n_x = number of Δx elements over which cutter interacts with rock formation
N = bit rotary speed (rev/min)
r = cutter compact radius (in)
r_w = parameter defined in Eq. 11i (in)
R = radial position of cutter compact center on bit (in)
ROP = bit rate of penetration (ft/hr)
T = bit drilling torque (ft-lbf)
T_f = downhole cooling fluid temperature (°F)
T_w = mean temperature across cutter wearflat (°F)
V = cutter speed with respect to rock (ft/sec)
V_r = volume of rock removed by a cutter (in^3)
ΔV_r = incremental volume of rock (in^3)
V_w = cutter wear volume associated with portion of wearflat in contact with rock (in^3)
$(V_w)_t$ = total cutter wear volume (in^3)
w = width of cutter wearflat at diamond face (in)
w_c = width of cut (in)
WOB = weight-on-bit (lbf)
WR = cutter wear ratio
x = coordinate along x-axis in hole coordinate system (in)
Δx = size of element along x-axis (in)
x' = coordinate along x-axis in bit coordinate system (in)
x_o = coordinate along x_o-axis in cutter profile coordinate system (in)
x'_o = coordinate along x'_o-axis in cutter coordinate system (in)
x_{bc} = x-coordinate of the bottom of cut in the center of the cut (in)
x_{c1} = x-coordinate of first point of contact between cutter and rock (in)
x_{c2} = x-coordinate of last point of contact between cutter and rock (in)
x_{w1} = x-coordinate of first end of cutter wearflat width (in)
x_{w2} = x-coordinate of second end of cutter wearflat width (in)
y = coordinate along y-axis in hole coordinate system (in)
y' = coordinate along y'-axis in bit coordinate system (in)
z = coordinate along z-axis in hole coordinate system (in)
z' = coordinate along z'-axis in bit coordinate system (in)
z_o = coordinate along z_o-axis in cutter profile coordinate system (in)
z'_o = coordinate along z'_o-axis in cutter coordinate system (in)
z_b = z-coordinate of the equivalent bottom of cut at a given x (in)
z_{bc} = z-coordinate of the bottom of cut in the center of the cut (in)
z'_{bc} = z'-coordinate of the bottom of cut in the center of the cut (in)
z_{c1} = z-value of first point of contact between cutter and rock (in)
z_{c2} = z-value of last point of contact between
z_{w1} = z-value of first end of cutter wearflat width (in)
z_{w2} = z-value of second end of cutter wearflat width (in)

β = cutter backrake angle (deg)
δ = depth of cut (in)
δ_e = effective depth of cut
Δ_i = distance from equivalent bottom of cut to rock surface at a given x (in)
θ = angular position of cutter compact center on bit (deg)
μ = friction coefficient between cutter and rock
μ_d = F_d/F = cutter drag coefficient
ρ_2 = rock density (lbm/ft^3)
ϕ_c = cutter inclination angle (deg)
ϕ_w = cutter wear angle in hole coordinate system (deg)
$(\phi_w)_o$ = cutter wear angle in cutter profile coordinate system (deg)
$(\phi_w)'_o$ = cutter wear angle in cutter coordinate system (deg)
χ_2 = rock thermal diffusivity (ft^2/hr)

subscripts

1 location 1, cutter 1
2 location 2
i ith Δx element over which cutter interacts with rock formation
j jth cutter
k kth cut
r reference cutter
$(.)_o$ coordinate expressed in terms of cutter profile coordinate system
$(\ )'_o$ coordinate expressed in terms of cutter coordinate system
$(\ )'$ coordinate expressed in terms of bit coordinate system

ACKNOWLEGMENT

This work was supported by the U.S. Department of Energy at Sandia National Laboratories under Contract DE-AC04-76DP00789. The assistance of D.L. Goodwin with the experimental work is gratefully acknowledged.

REFERENCES

1. Glowka, D.A. and Stone, C.M.: "Thermal Response of Polycrystalline Diamond Compact Cutters Under Simulated Downhole Conditions," SPEJ (April 1985) 143-156.

2. Glowka, D.A. and Stone, C.M.: "Effects of Thermal and Mechanical Loading on PDC Bit Life," SPE Drilling Eng. (June 1986) 201-214.

3. Glowka, D.A.: "Implications of Thermal Wear Phenomena for PDC Bit Design and Operation," SPE 14222, presented at 60th Ann. Tech. Conf. and Ex., Las Vegas, NV, Sept. 22-25, 1986.

4. Ortega, A. and Glowka, D.A.: "Studies of the Frictional Heating of Polycrystalline Diamond Compact Drag Tools During Rock Cutting," SAND80-2677, Sandia Natl. Lab., Albuquerque, NM, June 1982.

5. Ortega, A. and Glowka, D.A.: "Frictional Heating and Convective Cooling of Polycrystalline Diamond Drag Tools During Rock Cutting," SPEJ (April 1984) 121-128.

6. Melaugh, J.F. and Saltzer, J.A.: "Development of a Predictive Model for Drilling Pressurized Shale with Stratapax Blank Bits," presented at ASME Energy Technology Conf., Houston, TX, Jan. 19-22, 1981.

7. Kelsey, J.R., ed: "Geothermal Technology Development Program Annual Progress Report, October 1983-September 1984," SAND85-1138, Sandia Natl. Lab., Albuquerque, NM, Aug. 1985.

8. Cortes, J. and Besson, A.: "Behavior of Polycrystalline Diamond Compact Cutters While Drilling in Bottomhole Conditions-Field Applications," Proc. Int. Conf. on Geothermal Drilling and Completion Tech., SAND81-0036C, Sandia Natl. Lab., Albuquerque, NM, Jan. 21-23, 1981.

9. Walker, B., Drilling Research Lab., Salt Lake City, UT, private communication, April 1986.

10. Hood, M.: "A Study of Methods to Improve the Performance of Drag Bits Used to Cut Hard Rock," Report 35/77, Chamber of Mines of South Africa (Aug. 1977).

11. Hood, M.: "Cutting Strong Rock with a Drag Bit Assisted by High-Pressure Water Jets," J. South African Inst. Min. Met. (Nov. 1976) 79-90.

12. Dubugnon, O.: "An Experimental Study of Water Assisted Drag Bit Cutting of Rocks," presented at 1st U.S. Water Jet Symp., Golden, CO, April 7-9, 1981.

13. Glowka, D.A.: "Design Considerations for a Hard-Rock PDC Drill Bit," Trans., Geothermal Res. Council (Aug. 1985) Vol. 9, 123-128.

14. Glowka, D.A.: "Development of a Method for Predicting the Performance and Wear of PDC Drill Bits," SAND86-1745, Sandia Natl. Lab., Albuquerque, NM, Aug. 1986.

15. Chahine, G.L., Genoux, P.F., Liu, H.L., and Johnson, V.E.: "Analytical and Experimental Study of Self-Resonating Water Jets: Nozzle-Jet and Wall-Jet Interactions," SAND86-7124, Sandia Natl. Lab., Albuquerque, NM, Aug. 1986.

16. Jones, I.R. and Edwards, D.H.: "An Experimental Study of the Forces Generated by the Collapse of Transient Cavities in Water," J. Fluid Mech., Vol. 7 (1960) 596-609.

17. Johnson, V.E., Lindenmuth, W.T., Chahine, G.L., Conn, A.F., and Frederick, G.S.: "Research and Development of Improved Cavitating Jets for Deep-Hole Drilling," SAND83-7461, Sandia Natl. Lab., Albuquerque, NM, Jan, 1984.

18. Hibbs, L.E. and Sogolan, G.C.: "Wear Mechanisms for Polycrstalline Diamond Compacts as Utilized for Drilling in Geothermal Environments-Final Report," SAND82-7213, Sandia Natl. Lab., Albuquerque, NM, May 1983.

19. Aronson, E.A., McCaughey, K.G., and Walton, E.L.: "STRATAPAX Computer Program Update," SAND82-1087, Sandia Natl. Lab., Albuquerque, NM, Sept. 1982.

20. Kelsey, J.R., ed.: "Geothermal Technology Development Program Annual Progress Report, October 1980-September 1981," SAND81-2124, Sandia Natl. Lab., Albuquerque, NM, Sept. 1982.

21. Gill, C.W. and Martin, J.L.: "Matrix Body PDC Bits Prove Most Cost Effective in the Powder River Basin," IADC/SPE 13462, IADC/SPE 1985 Drilling Conference, New Orleans, LA, March 1985, 341-354.

APPENDIX A

Four coordinate systems are used to describe the cut and cutter profiles, as shown in Figure A-1. The hole coordinate system (x,y,z) is a non-rotating cartesian coordinate system whose z-axis is parallel to the longitudinal axis of the hole. The bit coordinate system (x',y',z') is a cartesian coordinate system which rotates and advances with the bit and which has a z'-axis parallel to the longitudinal axis of the bit and the z-axis of the hole coordinate system. The cutter coordinate system (x'_o,z'_o) is a two-dimensional, rectangular coordinate system that lies in the plane of each circular diamond face of the cutter. The cutter profile coordinate system (x_o,z_o) is the projection of the cutter coordinate system onto a radial plane that lies in the x,z plane of the hole coordinate system.

A point (x'_o,z'_o) in the cutter coordinate system is projected into the cutter profile coordinate system (x_o,z_o) as

$$x_o = x'_o \tag{A-1}$$

$$z_o = z'_o \cos \beta \ , \tag{A-2}$$

where β is the cutter backrake angle. The circular edge of a sharp cutter in the cutter coordinate system is described by the equation:

$$\left(\frac{x'_o}{r}\right)^2 + \left(\frac{z'_o}{r}\right)^2 = 1 \ , \tag{A-3}$$

where r is the radius of the circular cutter compact. Transforming this equation to the cutter profile coordinate system, the cutter profile proves to be one of an ellipse:

$$\left(\frac{x_o}{r}\right)^2 + \left(\frac{z_o}{b}\right)^2 = 1 \ , \tag{A-4}$$

where

$$b = r \cos \beta \ . \tag{A-5}$$

During one revolution of the bit, each cutter passes through the x-z plane of the hole coordinate system. As each cutter passes through this plane, the transformation equations between the hole coordinate system (x,y,z) and that cutter's profile coordinate system (x_o,z_o) are:

$$x = R + x_o \cos \phi_c + z_o \sin \phi_c \tag{A-6}$$

$$y = 0 \tag{A-7}$$

and

$$z = H - x_o \sin \phi_c + z_o \cos \phi_c \quad , \qquad \text{(A-8)}$$

where $$H = H' + f_r(360 - \theta)/360 \quad . \qquad \text{(A-9)}$$

Here R and H' are the radial and longitudinal locations, respectively, of the center of the cutter compact on the bit body. The parameter H, defined as the cutting height of the cutter, accounts for the fact that the bit advances in the z-direction as it rotates. This height, which is the z-coordinate of the center of each cutter as it passes through the x-z plane is a function of the feed per revolution, f_r, and the angular position, θ, of the cutter on the bit face. The angular position is defined as positive in the counterclockwise direction when viewing the face of the bit (see Fig. 17). The feed rate is related to the penetration rate and bit rotary speed with the equation

$$f_r = ROP/N \quad , \qquad \text{(A-10)}$$

where ROP is the rate of penetration and N is the bit rotary speed.

Combining Eqs. A-4 through A-8, we obtain the cutting profile (x,y,z) of a sharp cutter in terms of the hole coordinate system (Eq. 14).

Wear modifies the cutting profile according to the wearflat width, w, and the radial wear angle, ϕ_w. An algorithm in the program iterates upon the wear angle by initially assuming $\phi_w = \phi_c$. The cut profiles for each cutter are computed, and ϕ_w is calculated using Eq. 10. Since the new estimate of ϕ_w may be different from the initial guess, the wearflat locations on the cutters may change from the previous iteration, which in turn changes the cut profiles. The process is repeated until the solution converges for all cutters.

The cutter wearflat is easiest described in the cutter coordinate system. In this system, the wear angle $(\phi_w)'_o$ is related to the wear angle ϕ_w in the hole coordinate system with the equation

$$(\phi_w)'_o = \tan^{-1}\left[\frac{(z_{c1})'_o - (z_{c2})'_o}{(x_{c2})'_o - (x_{c1})'_o}\right] = \tan^{-1}\left[\frac{((z_{c1})_o - (z_{c2})_o)/\cos\beta}{(x_{c2})_o - (x_{c1})_o}\right] \quad , \qquad \text{(A-11)}$$

which leads to Eqs. 11j and 11k. The wearflat width, w, is measured in the cutter coordinate system. In the circular geometry of this sytem, geometric considerations give the results shown in Eqs. 11e-h. Eqs. A-6 and A-8 are then used to produce Eqs. 11a-d.

It should be noted that in cases where the wearflat develops on the side of the cutter ($\phi_w \neq \phi_c$), some inaccuracies in computed cutter forces will occur. This is caused by the fact that in such cases, the angular transformation converts some of the cutter backrake to a small effective siderake angle. This factor is not considered to be significant for the relatively small backrake angles generally used in PDC bits ($<30^o$).

TABLE I
DIMENSIONS OF CUTTER WEARFLATS USED IN SINGLE-CUTTER TESTS

CUTTER	A_w (in^2)	w (in)	L (in)	COMPACT DIAMETER (in)	WEARFLAT TYPE *
A	0.016	0.220	0.090	0.50	F
B	0.017	0.240	0.070	0.50	F
C	0.017	0.340	0.050	0.50	F
D	0.020	0.320	0.100	0.75	L
E	0.022	0.220	0.140	0.50	F,L
F	0.030-0.040	0.300-0.320	0.140-0.180	0.50	M,L
G	0.032	0.360	0.130	0.75	L
H**	0.029	0.340	0.120	0.75	L
I	0.040	0.320	0.180	0.50	M

* F = field worn; L = lab worn; M = machine ground.
** Cutter H used in waterjet-assisted cuts.

TABLE II
COEFFICIENTS IN EQS. 39 AND 40

COMPACT DIAMETER (in)	C_4 (in^{1-3n4})	n4	C_5 (in^{1-2n5})	n5
0.50	2.94	0.40	1.59	0.68
0.75	2.72	0.40	1.38	0.68

TABLE III
CUTTER POSITIONS IN BASELINE ANALYSIS

CUTTER	R (in)	θ (deg)	H' (in)
1	0.350	0.0	0.625
2	0.800	215.0	0.760
3	1.250	110.0	0.895
4	1.600	45.0	1.000
5	1.950	285.0	1.000
6	2.300	165.0	1.000
7	2.495	0.0	0.990
8	2.635	240.0	0.970
9	2.775	120.0	0.940
10	2.915	320.0	0.898
11	3.055	200.0	0.844
12	3.195	80.0	0.776
13	3.335	290.0	0.694
14	3.475	170.0	0.594
15	3.615	50.0	0.473
16	3.735	20.0	0.347
17	3.835	260.0	0.222
18	3.915	140.0	0.104
19	3.975	335.0	0.000
20	3.975	215.0	0.000
21	3.975	95.0	0.000

TABLE IV
BIT OPERATING CONDITIONS IN BASELINE ANALYSIS

PARAMETER	VALUE
Rock thermal conductivity, k_2	1.300 Btu/hr ft ^oF
Rock thermal diffusivity, X_2	0.033 ft^2/hr
Rock-cutter friction coefficient, μ	0.070
Worn cutter drag coefficient, μ_d	0.550
Sharp cutter drag coeffcient, μ_d	0.750
Worn Type A cutter (no jets) correlation constant, C_1	1.34 X 10^5 psi/$in^{0.42}$
Worn Type A cutter (no jets) correlation exponent, $n1$	0.42
Worn Type B cutter (w/jets) correlation constant, C_1	3.26 X 10^5 psi/$in^{0.93}$
Worn Type B cutter (w/jets) correlation exponents, $n1$	0.93
Sharp Type A cutter (no jets) correlation constant, C_2	2.55 X 10^4 lbf/$in^{1.64}$
Sharp Type A cutter (no jets) correlation exponent, $n2$	1.64
Sharp Type B cutter (w/jets) correlation constant, C_2	2.55 X 10^4 lbf/$in^{1.64}$
Sharp Type B cutter (w/jets) correlation exponent, $n2$	1.64
Abrasive Wear constant, C_6	6.89 X 10^{-13} in^2/lbf
Bit rotary speed, N	100 RPM
Downhole cooling fluid temperature, T_f	80 ^oF
Specified bit penetration rates, ROP	10,20,30,40,50 ft/hr

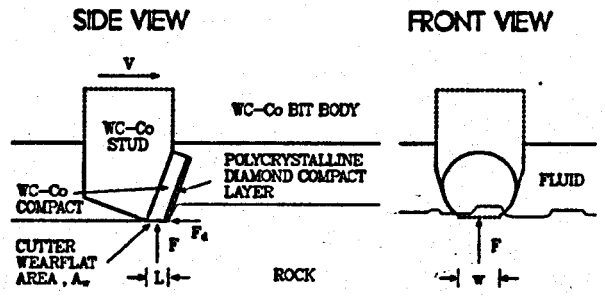

Fig. 1 - Geometry of a single cutter mounted on the leading face of a PDC bit and experiencing interaction with nearby cutters.

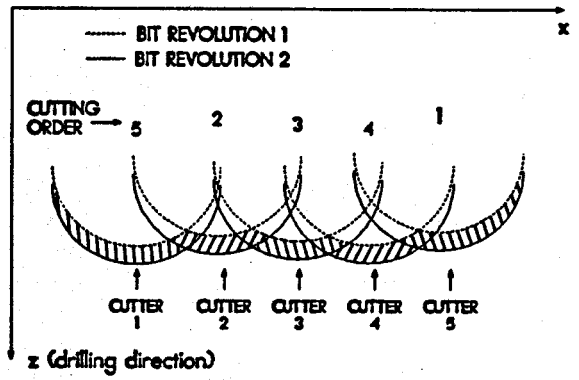

Fig. 2 - Cutting edge profiles for sharp cutters on the leading face of a PDC bit. Shaded areas represent cross-sectional areas of cut.

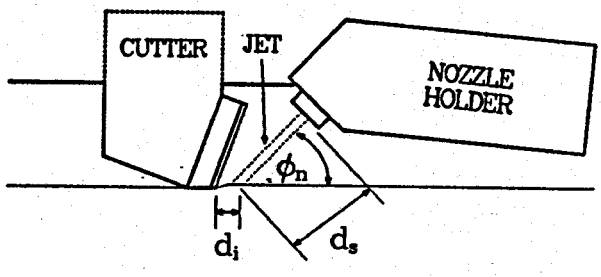

Fig. 3 - Geometry of single-cutter tests with waterjet assistance. Values used in test: d_j=0.1 in; d_s=1.65 in; ϕ_n=45°.

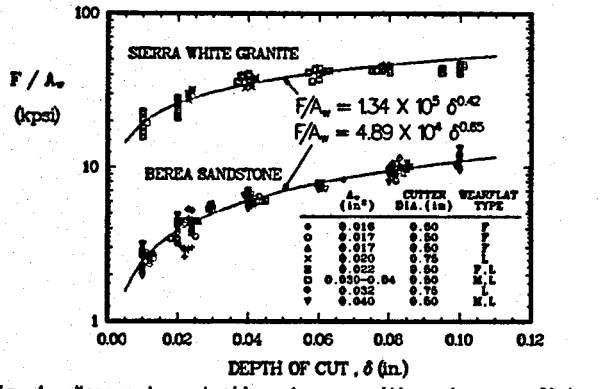

Fig. 4 - Measured penetrating stresses with various wearflat configurations in dry, non-interacting cuts. Wearflat type F=field worn; L=lab worn; M=machine ground.

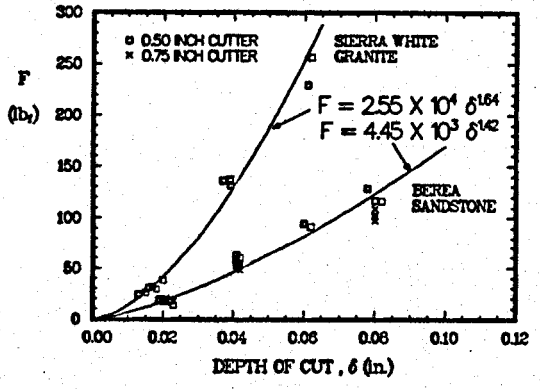

Fig. 5 - Measured penetrating forces with sharp cutters in dry, non-interacting cuts.

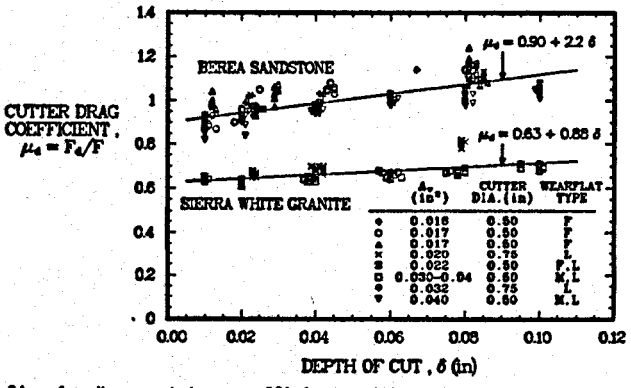

Fig. 6 - Measured drag coefficients with various wearflat configurations in dry, non-interacting cuts. Wearflat type described in Fig. 4 caption.

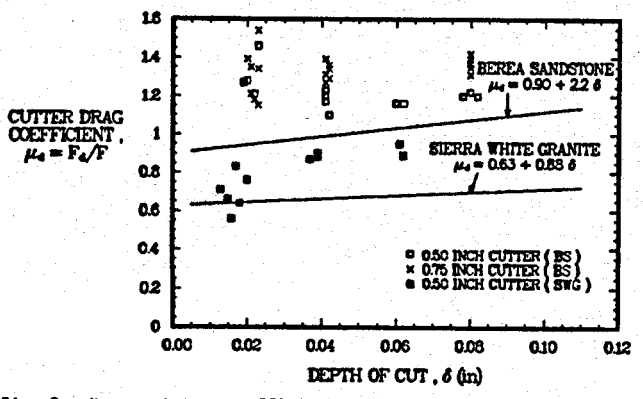

Fig. 7 - Measured drag coefficients with sharp cutters in dry, non-interacting cuts. Curves respresent mean data obtained with worn cutters (Fig. 6).

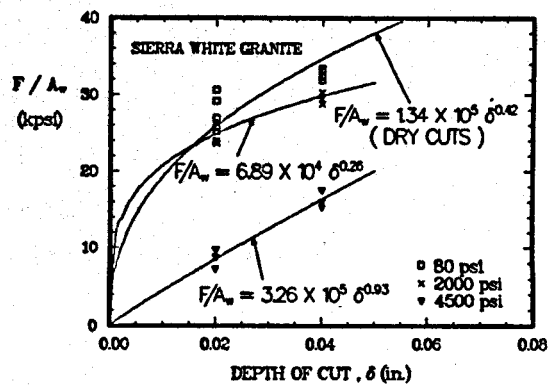

Fig. 8 - Measured penetrating stresses in non-interacting cuts made with jet assistance. Upper curve represents mean data from dry cuts (Fig. 4).

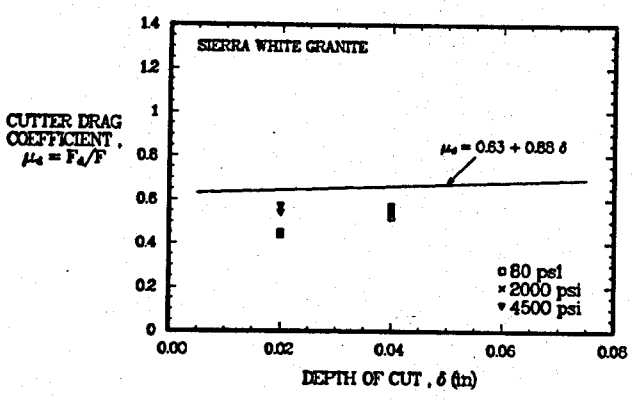

Fig. 9 - Measured drag coefficients in non-interacting cuts made with waterjet assistance. Curve represents mean data from dry cuts (Fig. 6).

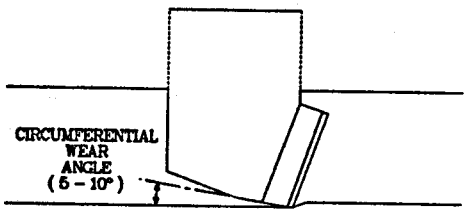

Fig. 10 - Circumferential wear angle found to develop on field-worn cutters.

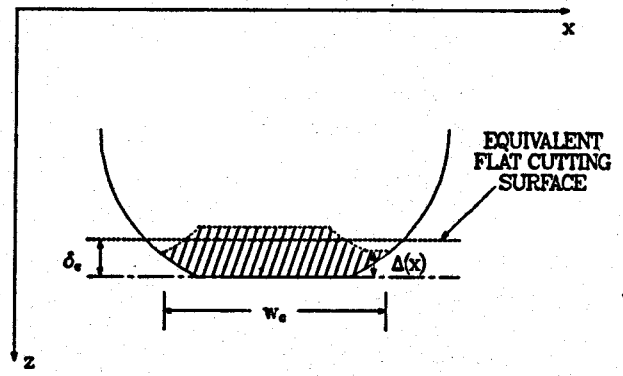

Fig. 11 - Typical cutting pattern for a worn cutter on the leading face of a PDC bit. Shaded area is actual cross-sectional area of cut.

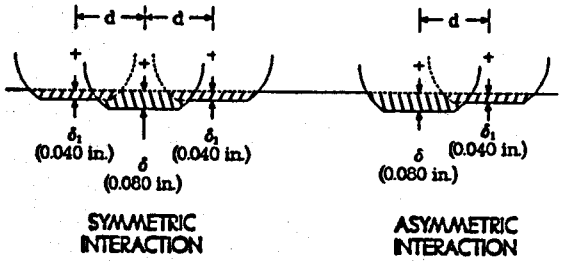

Fig. 12 - Cutting patterns used to simulate cutter interaction in Ref. 3. Test cut is the 0.080 inch cut in each pattern.

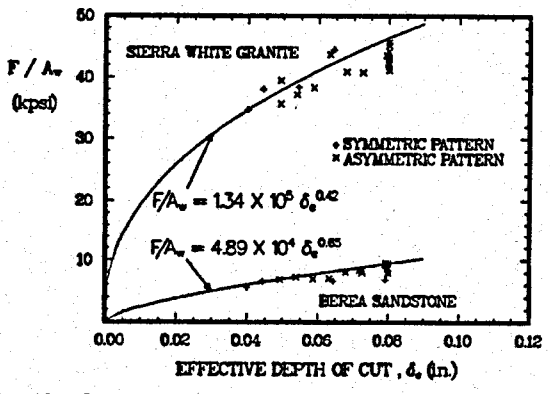

Fig. 13 - Predicted and measured penetrating stresses for dry, interacting cut tests conducted in Ref. 3.

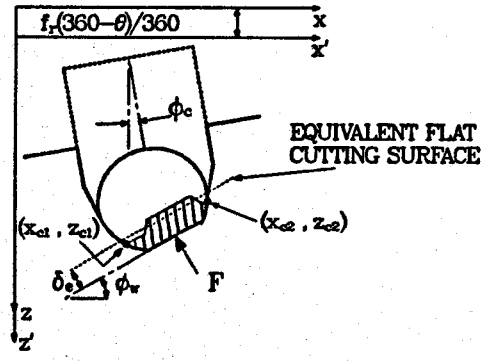

Fig. 14 - Cut and cutter profiles for a general PDC cutter. (x,y,z coordinate system is stationary; x',y',z' coordinate system travels with bit)

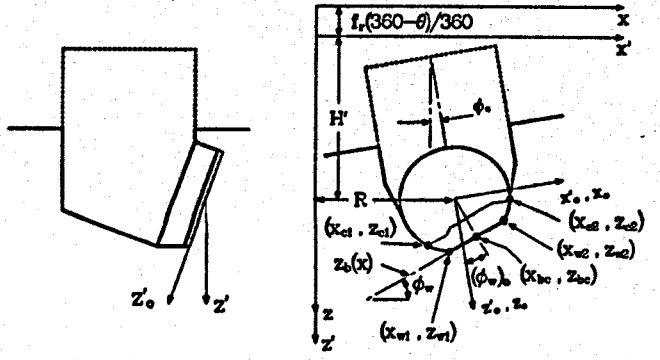

Fig. 15 - Cut and cutter profiles for a general PDC cutter, showing parameters used to compute profiles.

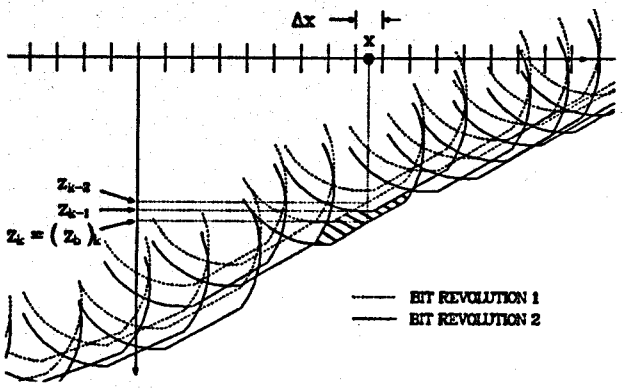

Fig. 16 - Schematic of algorithm used to compute z-coordinates of cutting profiles at each value of x.

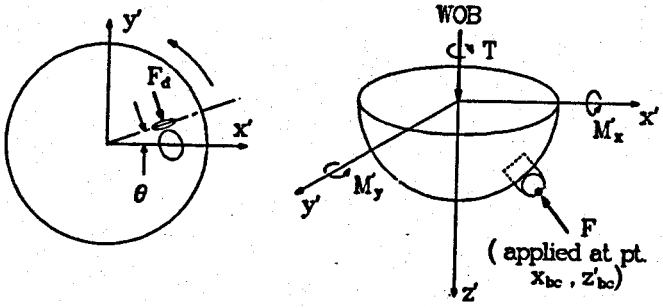

Fig. 17 - Schematic showing how cutter forces are integrated to produce bit performance parameters.

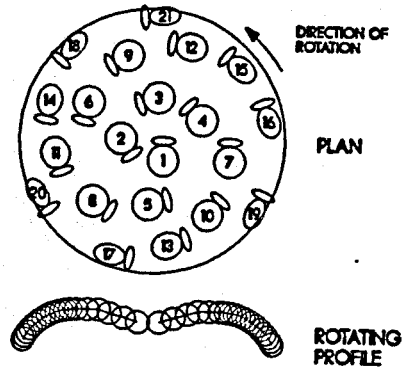

Fig. 18 - Schematic of 8-1/2" bit design considered in baseline analysis.

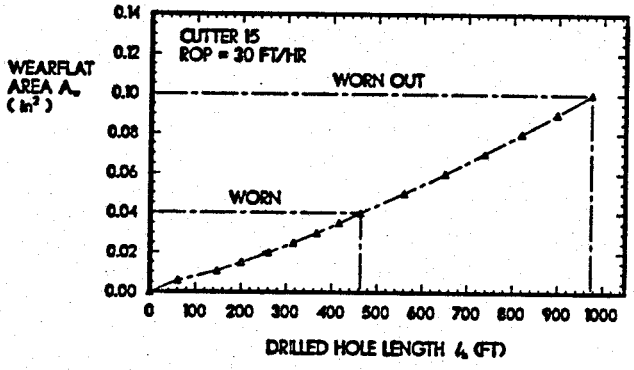

Fig. 19 - Growth of wearflat with highest wear rate in baseline analysis.

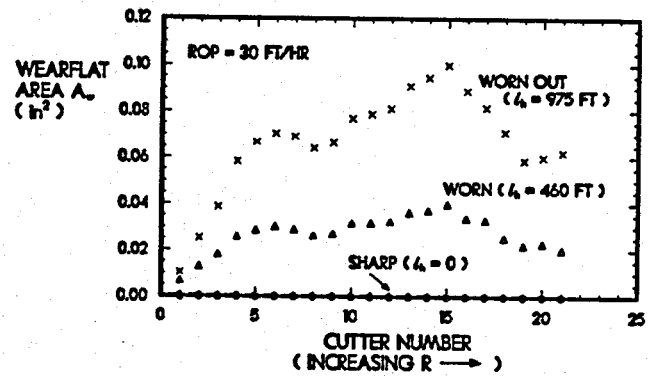

Fig. 20 - Predicted wear distribution across bit in baseline analysis at designated stages of wear.

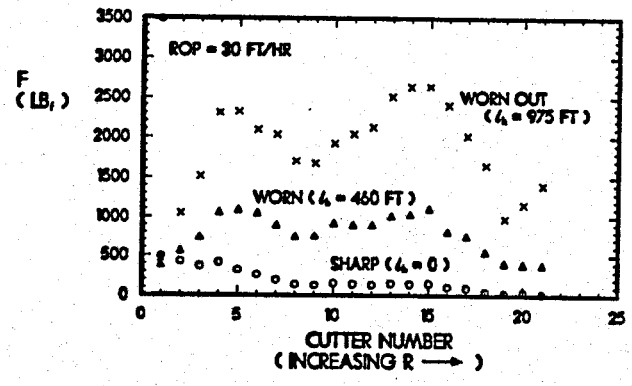

Fig. 21 - Predicted cutter penetrating forces in baseline analysis.

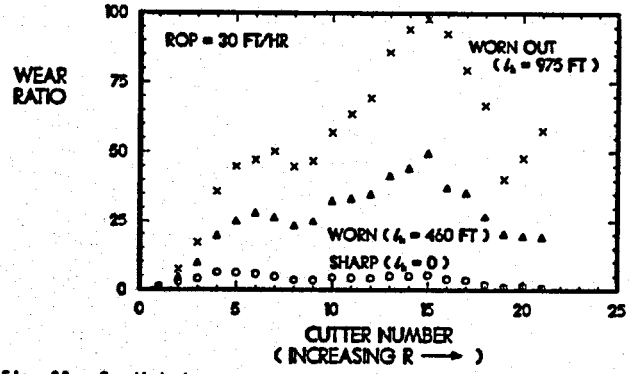

Fig. 22 - Predicted cutter wear ratios in baseline analysis (wear ratio = 1 for cutter 1).

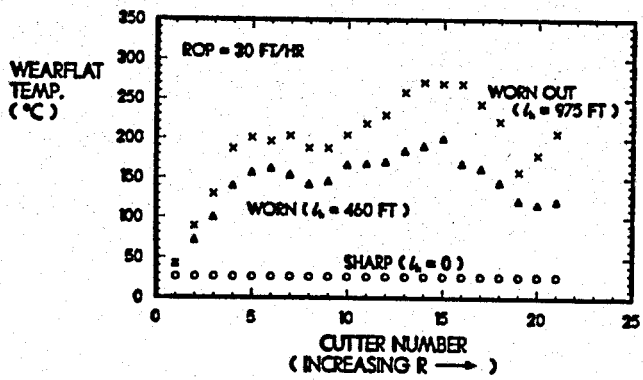

Fig. 23 - Predicted cutter wearflat temperature in baseline analysis.

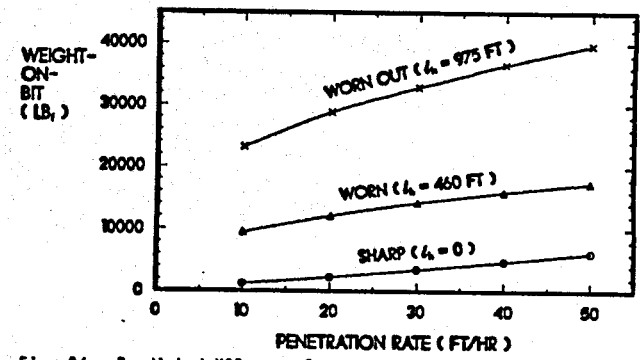

Fig. 24 - Predicted WOB as a function of specified ROP in baseline analysis.

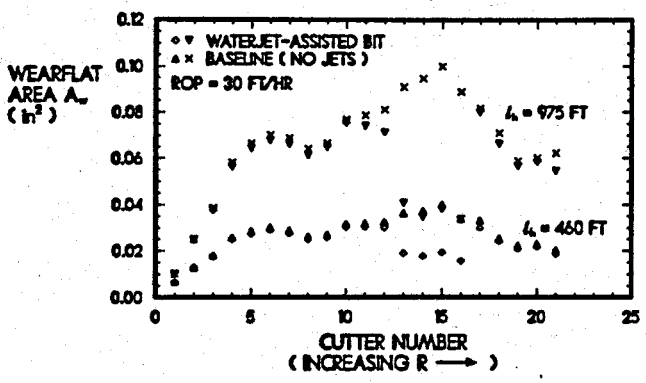

Fig. 33 - Predicted wear distribution across bit, showing effects of 4500 psi waterjet assistance to cutters 13-16.

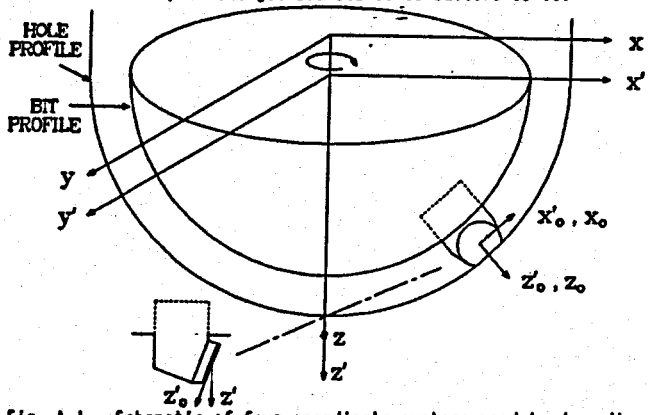

Fig. A-1 - Schematic of four coordinate systems used to describe cut and cutter profiles. Hole (x,y,z), bit (x',y',z'), cutter (x'_0,z'_0), and cutter profile (x_0,z_0) coordinate systems.

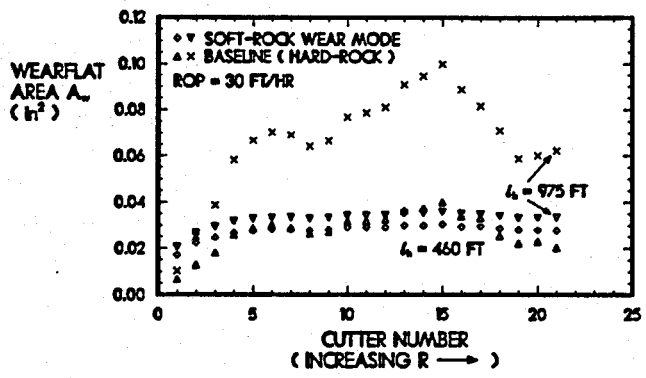

Fig. 34 - Predicted wear distribution across bit, showing effects of wear mode.

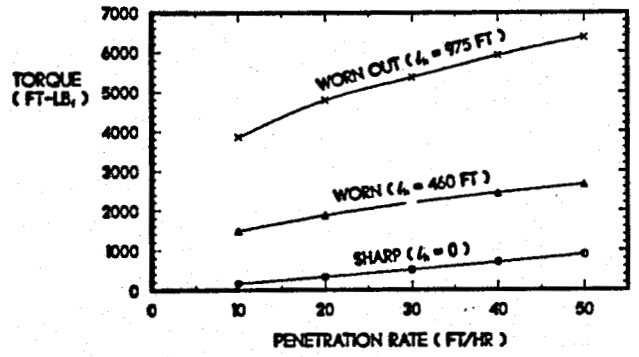

Fig. 25 - Predicted drilling torque as a function of specified ROP in baseline analysis.

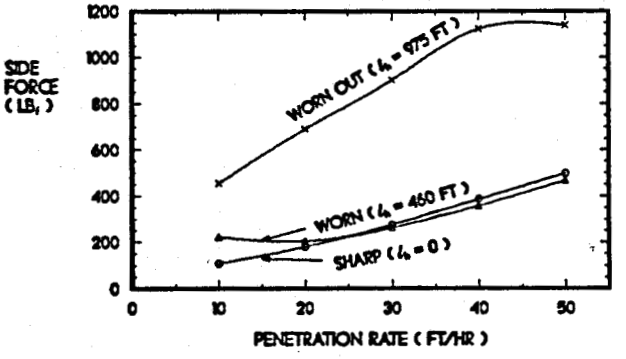

Fig. 26 - Predicted bit side force as a function of specified ROP in baseline analysis.

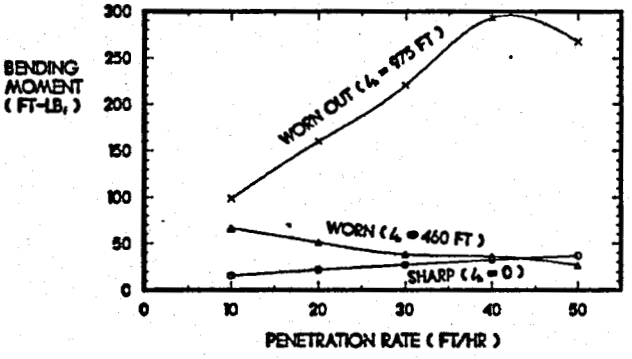

Fig. 27 - Predicted bit bending moment as a function of specified ROP in baseline analysis.

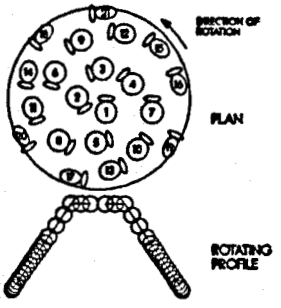

Fig. 28 - Schematic of bullet-nose bit used to demonstrate effects of bit profile.

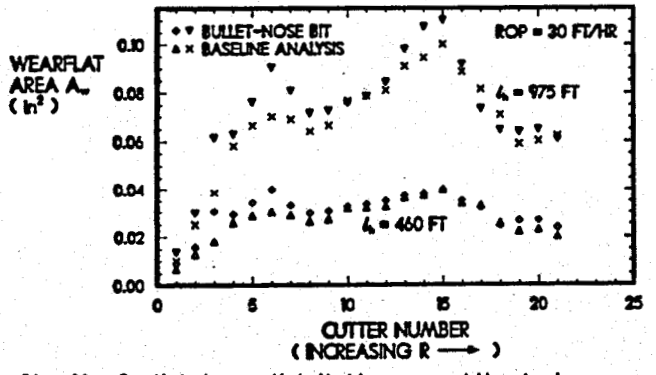

Fig. 29 - Predicted wear distribution across bit, showing effects of bit profile.

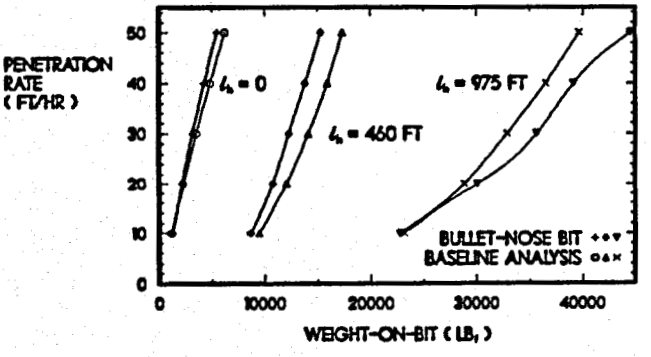

Fig. 30 - Specified ROP plotted as a function of predicted WOB to illustrate the effects of bit profile.

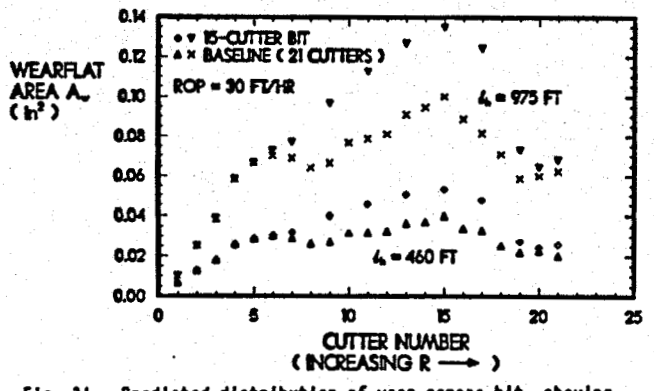

Fig. 31 - Predicted distribution of wear across bit, showing effects of cutter density.

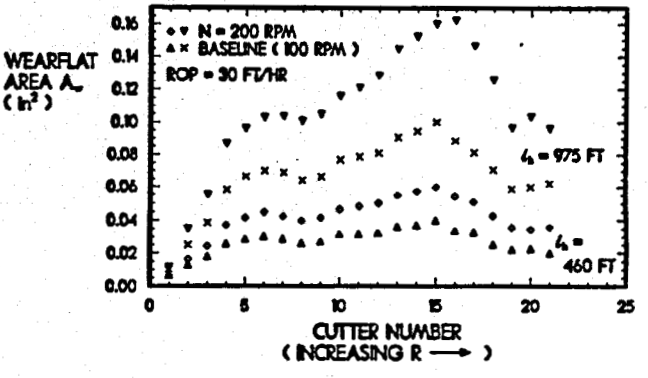

Fig. 32 - Predicted wear distribution across bit, showing effects of rotary speed.